Tectonic evolution of the Northeastern South China Sea from seismic interpretation

Yi-Ching Yeh,[1,2] Jean-Claude Sibuet,[3] Shu-Kun Hsu,[1] and Char-Shine Liu[4]

[1]   We interpret a grid of 2-D seismic reflection profiles to resolve the tectonic evolution of the northeastern South China Sea (SCS), identifying two significant postbreakup events, T1 and T2, which occurred before the end of the SCS opening. In the absence of the drilling data in the deep basin, we date these two events using the identification of the magnetic anomalies, the age of major unconformities at Ocean Drilling Program Site 1148 drilled on the northeastern SCS margin, and the age of basalt samples in the deep SCS. The tectonic phase T1 is a slight tensional tectonic event which occurred in the deep SCS, south of the Luzon-Ryukyu Transform Plate Boundary (LRTPB). It is characterized by oceanic tilted blocks and fan-shaped deposits, which developed 8–10 Myr after the onset of SCS seafloor spreading (37.8 Ma). It corresponds to the first ENE–WSW to E–W change in spreading direction, which occurred around chron C10 (~28.7 Ma). Event T2 is a magmatic phase observed in the deep SCS, south of the LRTPB. It is characterized by the uplift of former spreading features caused by an early Miocene (~22 Ma) magmatic phase, which is also recorded in north and south-central Taiwan.

1.   Introduction

[2]   The South China Sea (SCS) marginal basin opened from NE to SW in a complex tectonic process, starting during the middle Eocene and finishing near 15.5 Ma. Two hypotheses have been proposed to explain the opening. According to one model, Dangerous Grounds was pulled south by the subduction of the Proto-SCS plate under Palawan and Borneo, and moved along a right lateral strike-slip fault east of Vietnam [*Clift et al.*, 2008; *Taylor and Hayes*, 1980]. The opening ceased when the subduction jammed and Dangerous Grounds collided with Palawan. According to the other model, the southern motion of Dangerous Grounds was linked to that of Borneo and Indochina and proceeded to the extrusion of Indochina as a consequence of the India-Eurasia collision. The western boundary of the basin was the prolongation of the Red River fault and was a left lateral transform fault [*Briais et al.*, 1993; *Peltzer and Tapponnier*, 1988; *Tapponnier et al.*, 1982].

[3]   A Dangerous Grounds plate motion with respect to Eurasia around a pole of rotation located to the west of Dangerous Grounds may explain the southwestward SCS progressive opening from chron C12 (31 Ma) in the east to 15.5 Ma [*Briais et al.*, 1993]. In the northeastern SCS, *Hsu et al.* [2004] identified chron C15 (35 Ma) to chron C17 (37.8 Ma), suggesting that the northeastern SCS is much older than the rest of the SCS. Whether this domain was formed in the same way as the rest of the SCS is still not clear. In the extreme northeastern SCS, between the Luzon-Ryukyu Transform Plate Boundary (LRTPB) and the Manila trench, a small triangular portion of old oceanic domain, lying 800 m deeper than the rest of the SCS with only three magnetic lineations. It is difficult to date them. This domain may be part of the Proto-SCS plate or part of western Philippine sea plate [*Sibuet et al.*, 2002].

[4]   In this paper, we interpret new magnetic lineations between chrons C15 (35 Ma) and C12 (31 Ma), multi-channel seismic (MCS) data and a wide-angle reflection seismic profile to classify the crust located southwest of the LRTPB as thick oceanic crust and not thinned continental crust intruded by volcanics as suggested by *Wang et al.* [2006]. Newly acquired MCS data show that a tectonic event and a magmatic event have imprinted on both the oceanic basement and the overlying sediments.

2.   Magnetic Anomalies and Nature of the Crust

[5]   We use the *Gradstein et al.* [2004] geomagnetic reversal time scale to date the magnetic lineations. This time scale does not differ significantly for late Cenozoic ages from the *LaBrecque et al.* [1977] time scale used by *Taylor*

[1]Institute of Geophysics, National Central University, Chung-Li, Taiwan.
[2]Now at Department of Geology and Geophysics, University of Hawaii at Manoa, Honolulu, Hawaii, USA.
[3]Institute of Applied Geosciences, National Taiwan Ocean University, Keelung, Taiwan.
[4]Institute of Oceanography, National Taiwan University, Taipei, Taiwan.
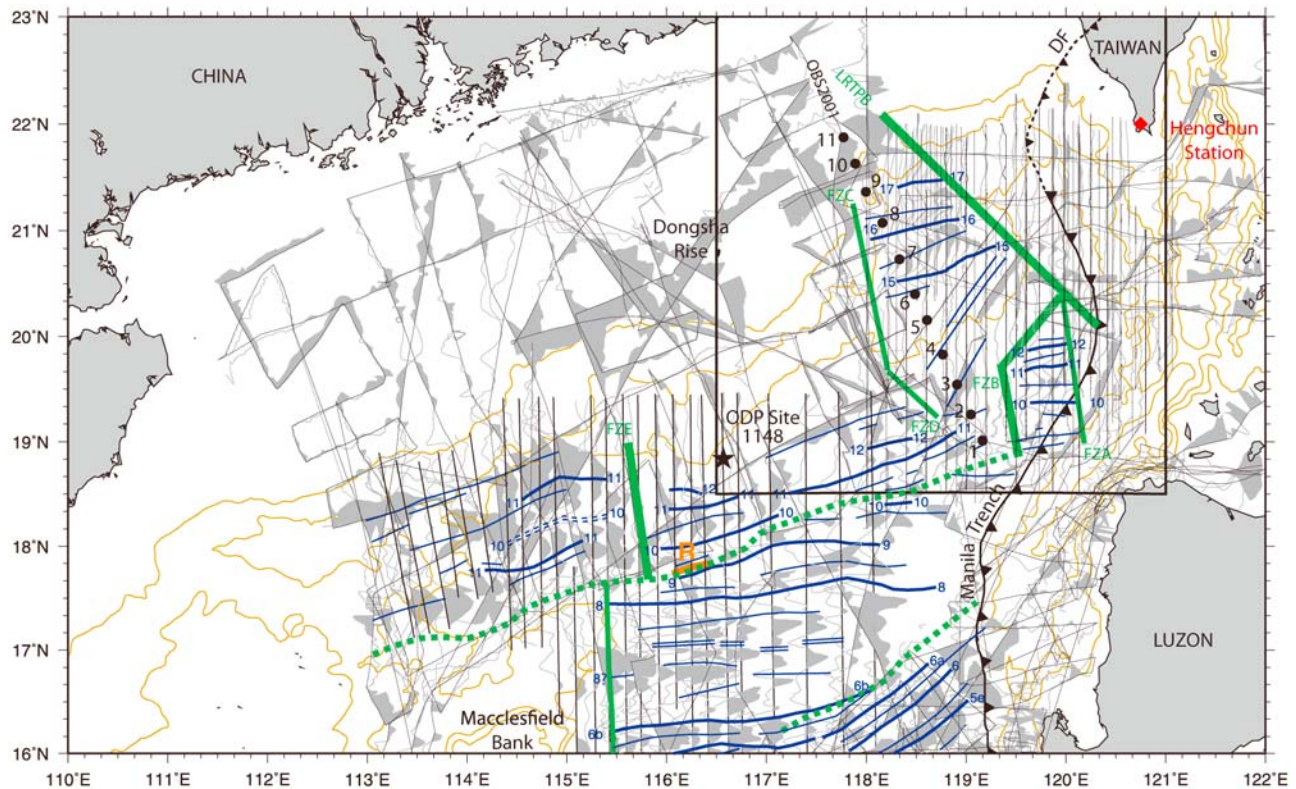
Figure 1. Magnetic anomalies profiles projected perpendicularly to the track lines. Positive magnetic anomalies are plotted in gray. Brown lines show simplified bathymetry every kilometer. Bold blue lines, magnetic lineations and their identifications; thin blue lines, other magnetic lineations; double blue lines, failed rift axes. Thin green lines, fracture zones; thick green lines, plate boundaries; green dashed lines, changes in seafloor spreading directions at chrons C10-C11 and C6b-C7; LRTPB, Luzon-Ryukyu transform plate boundary; DF, deformation front. The large square box shows the detailed study area. Black dots numbered 1–11 are locations of ocean bottom seismometers (OBSs) along the OBS2001 refraction profile [*Wang et al.*, 2006].

and Hayes [1980, 1983], from the *Patriat* [1987] time scale used by *Briais et al.* [1993], or from the *Cande and Kent* [1995] time scale used for magnetic lineations identified in the northeastern SCS [*Hsu et al.*, 2004].

[6] N070° trending magnetic lineations were first recognized close to the Manila trench by *Bowin et al.* [1978]. The first correlation of magnetic data with a geomagnetic reversal time scale was proposed by *Taylor and Hayes* [1980, 1983], who identified magnetic lineations from chron C11 (30.1 Ma) to C5d (17.6 Ma). Combining data from *Chen* [1987] with magnetic data acquired in the axial area of the SCS, *Briais et al.* [1993] concluded that seafloor spreading ceased 15.5 Ma ago in the SCS, after chron C5c (16.7 Ma). They also showed that spreading rates and directions of spreading changed at chron C10 (28.7 Ma) and C5d (17.6 Ma). More recently, *Barckhausen and Roeser* [2004] acquired five NW-SE oriented magnetic profiles across the SCS, between 112°E and 118°E. On the basis of forward modeling, they suggest that seafloor spreading ceased at chron 6A1 (20.5 Ma) instead of 15.5 Ma. As these magnetic lineations identifications are based on only five profiles oblique to SCS spreading direction and need to be confirmed, we do not use them in this paper. Magnetic data recently acquired in the northeastern SCS show the existence of E–W trending magnetic lineations modeled as chrons

C15 (35.0 Ma) to C17 (37.8 Ma) [*Hsu et al.*, 2004], confirming that the SCS spreading center propagated from NE to SW.

[7] Figure 1 shows magnetic anomalies projected perpendicularly to the track lines used in this study. Data come from the National Geophysical Data Center [*National Geophysical Data Center*, 2002], the Coordinating Committee for Geoscience Programmes in East and Southeast Asia (CCOP) magnetic database [*Geological Survey of Japan and Coordinating Committee for Geoscience Programmes in East and Southeast Asia*, 1994], *Chen* [1987], and *Sibuet et al.* [2002] as well as from numerous cruises of the Taiwanese oceanographic research vessels [*Hsu et al.*, 2004]. Magnetic anomalies were computed by using the 2005 International Geomagnetic Reference field corrections model [*Maus et al.*, 2005]. Diurnal corrections were performed for several Taiwanese cruises by using magnetic daily records from the Hengchun station in southern Taiwan (Figure 1). We have added ~30% more recently acquired magnetic profiles extracted from the NGDC and CCOP databases to the databases used by *Briais et al.* [1993] and *Hsu et al.* [2004].

[8] Basically, we have adopted the *Briais et al.* [1993] and *Hsu et al.* [2004] interpretations. With the newly available magnetic data, we have extended the trends of magnetic
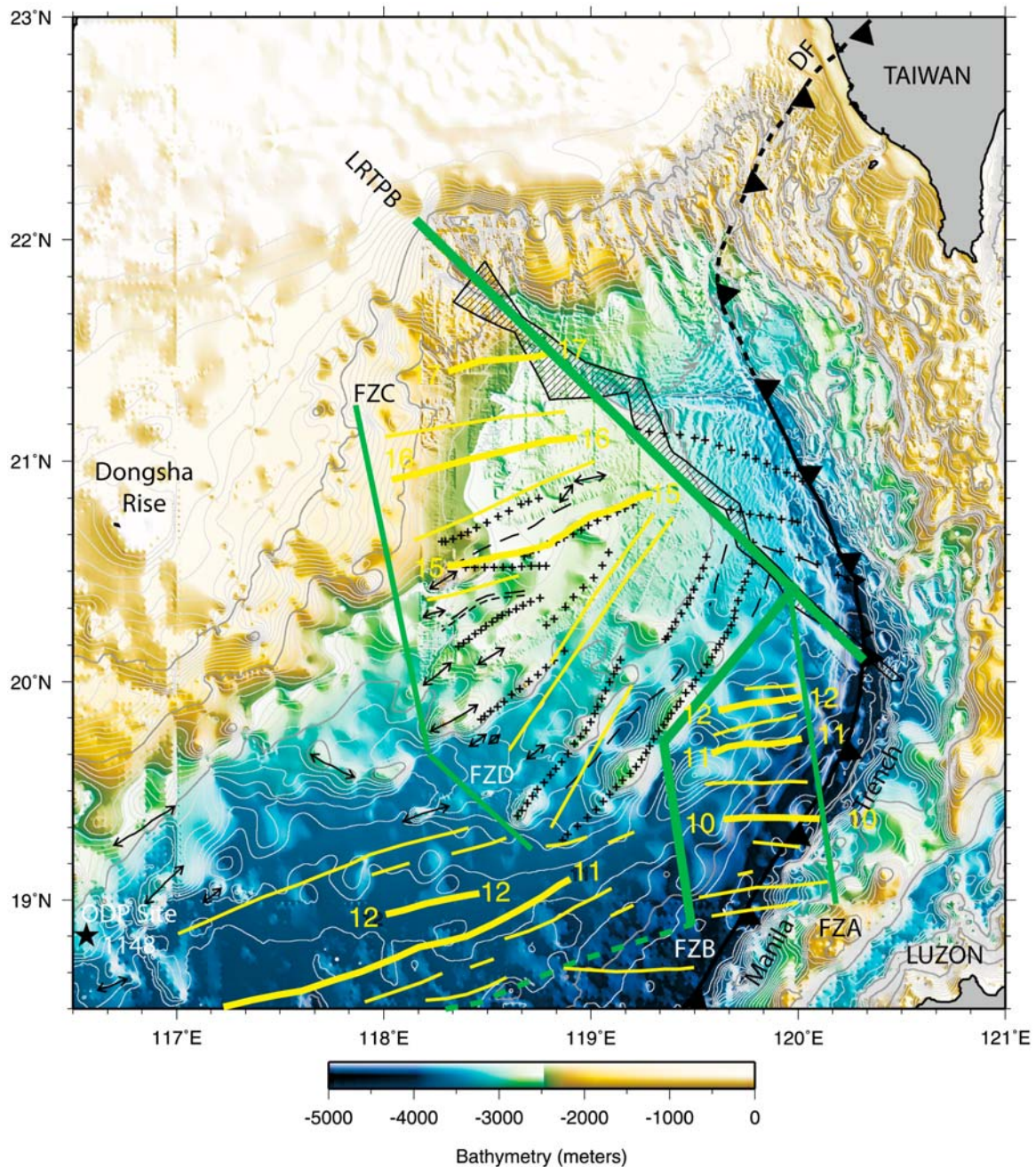
Figure 2. Bathymetric map [*Hsu et al.*, 2004] of the northeastern South China Sea (SCS). Available swath-bathymetric data have been merged with conventional echo sounder data. White thin lines, 100 m bathymetric contours. Bold yellow lines, identified magnetic lineations; thin and thick green lines, fracture zones (FZs) and plate boundaries, respectively; green dashed lines, changes in seafloor spreading directions; black crosses and dashed black lines, structural highs and depressions established from seismic data, respectively; black lines with double arrows, ridge axes determined from bathymetric data. The LRTPB is defined through the hachured area (acoustic basement expression of the plate boundary). DF, deformation front.

lineations, particularly in the northern corner of the SCS, and also have identified fracture zones (FZs), which limit the lateral extension of magnetic lineations. These FZs are represented as straight lines on Mercator projection because the precision in their drawing is not good enough to draw them as small circles. They are N352° oriented and generally follow free-air gravity anomaly trends [*Yeh*, 2006].

Between chrons C15 (35 Ma) and C12 (31 Ma), weak magnetic anomalies are aligned along the N035° direction (Figure 1). These magnetic lineations are parallel to a series of positive and negative free-air gravity anomaly lineations [*Yeh*, 2006] and bathymetric ridges (Figure 2). Because of the weak amplitudes and the reduced number of magnetic reversal events between C15 and C12, it is difficult to model
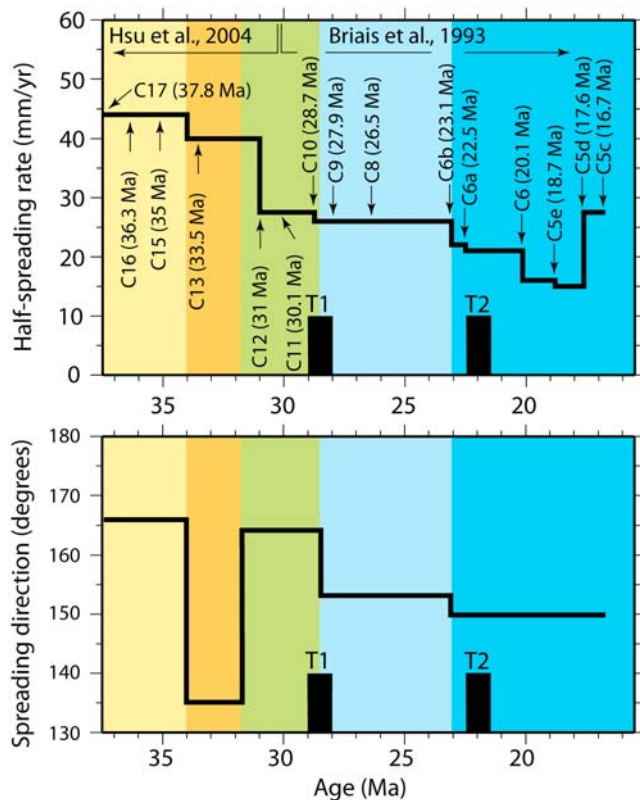
Figure 3. Half-spreading rates and directions of spreading in the northeastern SCS. (a) Half-spreading rates calculated from chron C17 to 15.5 Ma by using magnetic synthetic models between chrons C17 and C12 [*Hsu et al.*, 2004] and chrons C12 and C5c [*Briais et al.*, 1993] calculated using the *Gradstein et al.* [2004] time scale. T1 and T2 are the extensional tectonic phase and the magmatic event, which affected the northeastern SCS, south of the LRTPB. (b) Spreading directions are calculated by assuming that they are perpendicular to the trends of magnetic lineations. Note the large excursion of spreading rate between chrons C15− and C12+. Colors represent oceanic domains separated by significant changes in spreading rate, spreading direction or both: yellow, chron C17 to C15− oceanic domain formed perpendicularly to the direction of the continental margin north of the LRTPB with seafloor spreading extension at N166°; orange, chron C15− to C12+ oceanic domain formed during a short time with seafloor spreading extension at N135°; light green, chron C12+ to C9/C10 oceanic domain formed again perpendicularly to the direction of the continental margin north of the LRTPB with seafloor spreading extension at N164°; light blue, chron C9/C10 to C6b oceanic domain formed at N153°. Dark blue, chron C6b to 15.5 Ma oceanic domain formed at N150° in its western part and at N142° in its eastern part, suggesting that a rift axis readjustment occurred at chron C6b west of 117.5°E longitude.

and date them. However, by interpolation of the magnetic lineations identified to the north and to the south of these weak events, they should represent the C15− to C12+ sequence, though the characteristic C13 lineation was not recognized. These magnetic lineations do not have sym-metrical counterparts in the southern part of the SCS, as they already have been subducted beneath the Manila subduction zone, leaving the possibility of a ridge jump to explain the absence of C13 lineation.

[9] We observe two major changes in the direction of magnetic lineations: (1) The first change is from an ENE–WSW direction in the north to an E–W direction in the south between chrons C9 (27.9 Ma) and C11 (30.1 Ma). This change in direction does not appear in the map of magnetic lineations by *Briais et al.* [1993]. Note that this change in spreading direction does not correspond to a major change in spreading rate (Figure 3). (2) The second change in the direction of magnetic lineations occurs east of 117.5°E, from E–W trending chron C6b (23.1 Ma) to NE–SW trending chrons C6a (22.5 Ma) to C5c (16.7 Ma). This change of magnetic lineation was not obvious in the map of *Briais et al.* [1993], but corresponds to a 5 mm/yr decrease in half-spreading rate between chrons C6b and C6a (Figure 3). Half-spreading rates increase from 15 mm/yr to 27.5 mm/yr later at chron C5d (17.6 Ma), with the orien-tation of spreading segments changing from N070° to N050–040° [*Briais et al.*, 1993].

[10] *Briais et al.* [1993], based on the lack of magnetic data in the northeastern SCS, and *Lin et al.* [2003], based on stratigraphic subsidence data in the west Taiwan basins, independently interpreted the northeastern SCS as extended continental crust and dated the onset of oceanic spreading at chron 12 (31 Ma). However, *Hsu et al.* [2004] collected detailed magnetic data in the northeastern SCS and identi-fied magnetic lineations of oceanic origin created by sea-floor spreading processes. Only one wide-angle seismic experiment (OBS2001 in Figure 1) conducted in the northeastern SCS [*Wang et al.*, 2006] may help to charac-terize the nature of the crust. Figure 4a shows the interpre-tation of *Wang et al.* [2006] based, in the absence of crustal reflectors and Moho on MCS data, on their phase identifi-cations and forward modeling. For clarity, 1-D velocity profiles at each ocean bottom seismometer (OBS) location were plotted in Figure 4b as a function of depth below the top of the acoustic basement. Velocity bounds for the 59–127 Ma oceanic crust [*White et al.*, 1992], for the exhumed mantle [*Bullock and Minshull*, 2005] and the average velocity of extended continental crust [*Christensen and Mooney*, 1995] are also displayed. As shown by *Wang et al.* [2006], OBSs 10 and 11 are clearly located on extended continental crust. The crust beneath all the other OBSs was interpreted by *Wang et al.* [2006] as thinned continental crust intruded by volcanics (A to D in Figure 1a) overlying a 3-km-thick 6.9–7.2 km/s underplated layer, following *Yan et al.* [2001] interpretation's of a wide-angle seismic reflection experiment carried out on the northern SCS margin at 116°E.

[11] An alternative interpretation is to consider the crust as an abnormally 11-km-thick oceanic crust, as suggested by gravity modeling [*Hsu et al.*, 2004; *Yeh and Hsu*, 2004] and by the hummocky morphology of the acoustic basement [*Ku and Hsu*, 2009; *Tsai et al.*, 2004]. If this is true, following *Mutter and Mutter* [1993], a relatively high mantle tem-perature of 1340°C is required to emplace a 6-km-thick layer 2 with an average velocity of 5.7 km/s and a 5-km-thick layer 3 with an average velocity of 7.0 km/s. Such a simplified velocity structure is in agreement with OBSs 1–9
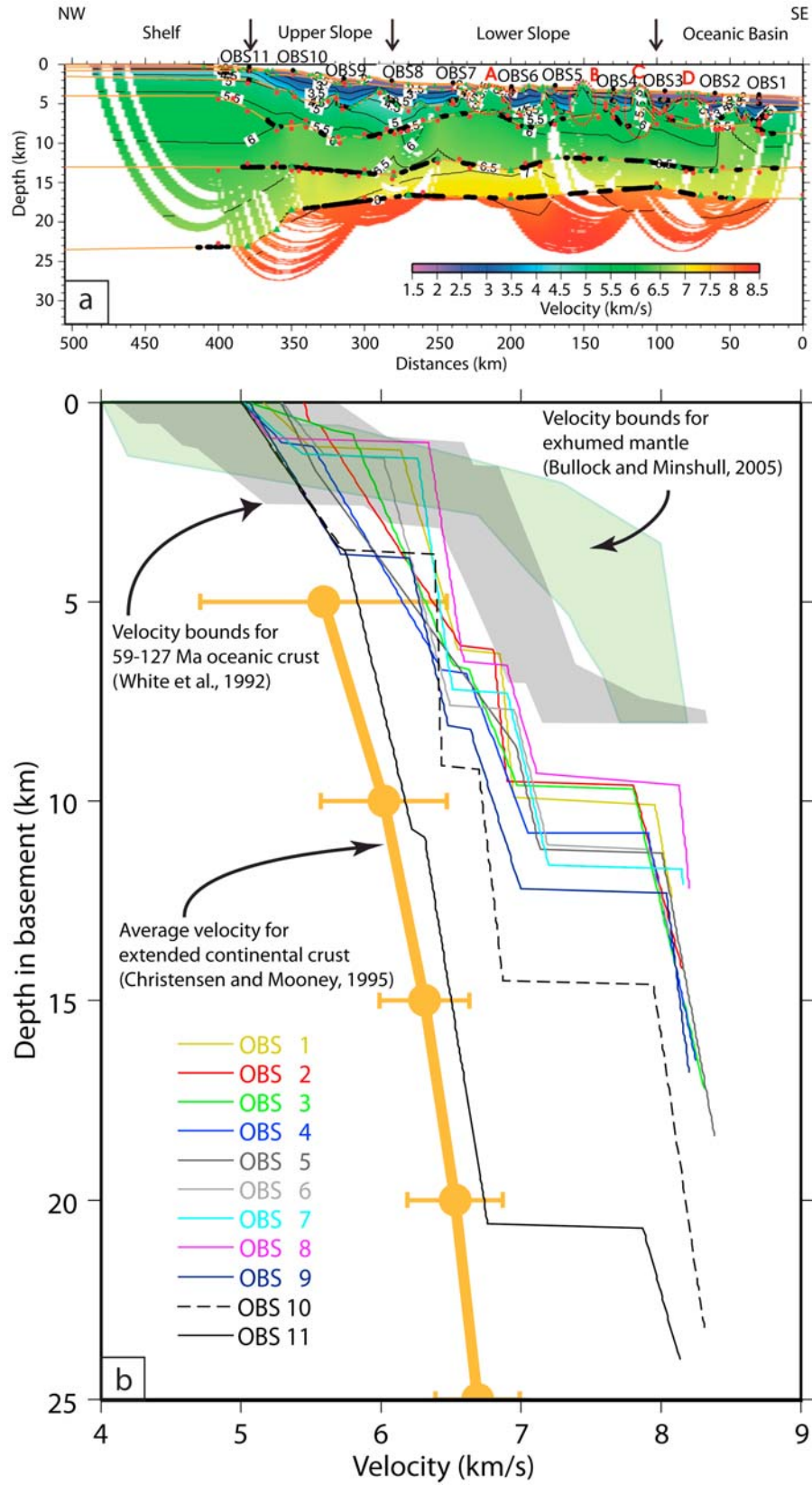
Figure 4

velocities (Figure 4b). However, there is no apparent boundary in the velocity profiles separating continental and oceanic crust.

[12] Thus, the seaward portion of the OBS2001 wide-angle seismic profile may be interpreted either as thinned continental crust intruded by volcanic features with magmatic underplating or as an abnormally thick oceanic crust. As the symmetrical part of this region is subducted beneath the Manila subduction zone, it is impossible to distinguish unambiguously between thick oceanic crust with symmetrical lineations and thinned continental crust intruded by asymmetrical volcanic ridges. The OBS2001 profile cuts across the N070° trending magnetic lineations C15 and C16 (Figure 1) characterized by large amplitude magnetic anomalies which can be continuously followed over distances of ~100 km. These magnetic lineations are oblique to the N035° trend of the adjacent continental margin. Though this argument is weak, it seems unlikely to emplace such long volcanic ridges within a thinned continental crust either during or after the rifting period at a significant angle with respect to the N035° trend of the continental margin. Therefore, we instead suggest the emplacement of an abnormally thick oceanic crust between the N035° trending continental margin and the LRTPB.

3. Multichannel Seismic Data Interpretation

3.1. Data Acquisition and Processing

[13] Figure 5 shows the track lines of MCS data collected in the northeastern SCS. Since the first MCS data collected in 1995 and 1996 by the R/V *Maurice Ewing* (four E–W profiles, 160 channels) and the R/V *L'Atalante* (eight profiles, six channels) [*Sibuet et al.*, 2002], four cruises were performed on the R/V *Ocean Researcher I*: MCS645 in 2002 (4 profiles, 24 channels), MCS654 in 2002 (1 profile, 48 channels), MCS689 in 2003 (4 profiles, 48 channels) [*Tsai et al.*, 2004; *Yeh and Hsu*, 2004], and MCS693 in 2003 (4 profiles, 48 channels) [*Ku and Hsu*, 2009]. In addition, the South China Sea Institute of Oceanology, China, collected three 48-channel profiles (MLTW, 97304Aa and Ab) in 2001 [*Tsai et al.*, 2004]. Except for the *Maurice Ewing* data, which were already processed, all other data were reprocessed through a band-pass filter of 8–16–32–64 Hz, true amplitude recovery, 1500 m/s constant velocity stacking, and 1500 m/s poststack F–K migration by using ProMAX software at the National Central University.

[14] Examples of portions of seismic profiles located in Figure 5 are shown in Figures 6–12. The acoustic basement horizon B and two acoustic unconformities (U1 and U2) onlapped by sedimentary layers have been identified. In the following sections, the acoustic basement and acoustic unconformities are associated with crustal provinces, a tensional tectonic phase, and a magmatic episode, respectively.

3.2. Acoustic Basement Horizon B

[15] The acoustic basement of the deep northeastern SCS is generally characterized by chaotic seismic reflections without any intrabasement reflectors (Figures 6–12). For example, Figures 6, 7, and 9 are portions of the MCS689-5 line along which the OBS2001 wide-angle seismic reflection line (Figure 4) was shot. The hummocky character of basement reflections is typical of oceanic crust rather than continental crust with intrusions, in agreement with the interpretations of *Ku and Hsu* [2009] and *Tsai et al.* [2004].

[16] Even though the sediment thickness in the northeastern SCS basin is at least 1 km [e.g., *Sibuet et al.*, 2002], the bathymetric map (Figure 2) displays a series of elongated ridges in the deep SCS basin. Figure 13 shows the contoured acoustic basement depth map. Ridges and troughs identified on seismic profiles have been interpolated from profile to profile and are marked by a series of crosses and dashed lines, respectively. They generally follow highs and lows of the contoured basement depth map, correspond to free-air gravity anomaly highs, and are superimposed on or parallel to the identified magnetic lineations, including where N035° trending magnetic lineations located between chrons C15− and C12+ have been identified. Three main domains are identified: (1) the northwest one characterized by ENE–WSW oriented magnetic anomalies belonging to the chrons C17 to C15 sequence [*Hsu et al.*, 2004]. This domain is bounded to the west by a fracture zone FZC, which roughly follows the change in direction of the segment of margin located east of Donghsa Rise. (2) The central domain formed between chrons C15− and C12+ is characterized by NE–SW oriented basement and magnetic trends, which are significantly oblique to all the older and younger basement and magnetic trends. A fracture zone FZD, presumably oriented perpendicularly to the magnetic trends, bounds this domain to the west. (3) Farther southeast, the basement deepens in the direction of the Manila trench. Owing to the southeastward basement deepening and increasing sediment thickness, basement ridges and troughs are difficult to identify, though they might be parallel to magnetic lineations C12 to C10.

[17] The LRTPB is a prominent morphotectonic feature, which was interpreted as a major former plate boundary between the SCS and the Philippines Sea or Proto-SCS plate [*Sibuet et al.*, 2002]. Northeast of the LRTPB, the oceanic basement deepening suggests a much older crust than that southwest of the LRTPB, even though the subductions of the Manila subduction zone and the former Ryukyu subduction zone, which extended southwest of Taiwan until 17–18 Ma [*Sibuet et al.*, 2004] may have deepened the basement in the direction of the trench. North of LRTPB, seismic data show the presence of three basement ridges associated with WNW–ESE oriented gravity and magnetic

Figure 4. (a) *P* wave velocity model along profile OBS2001, location shown in Figure 1 [*Wang et al.*, 2006]. Black dots, OBS locations with average spacing of 35 km. Velocity contours every 0.5 km/s. Buried and outcropping volcanic ridges (A to D) are enclosed by dotted red circles. (b) 1-D velocity-depth profiles across the northeastern SCS margin for each OBS every 35 km. The dark shaded region indicates the velocity bounds for normal oceanic crust aged 59–144 Ma [*White et al.*, 1992]; the light green region shows the bounds of velocity-depth profiles through the zone of exhumed mantle at West Iberia [*Bullock and Minshull*, 2005]; the orange thick line is the average velocity curve for extended continental crust with horizontal bars representing ±1 standard deviation [*Christensen and Mooney*, 1995].
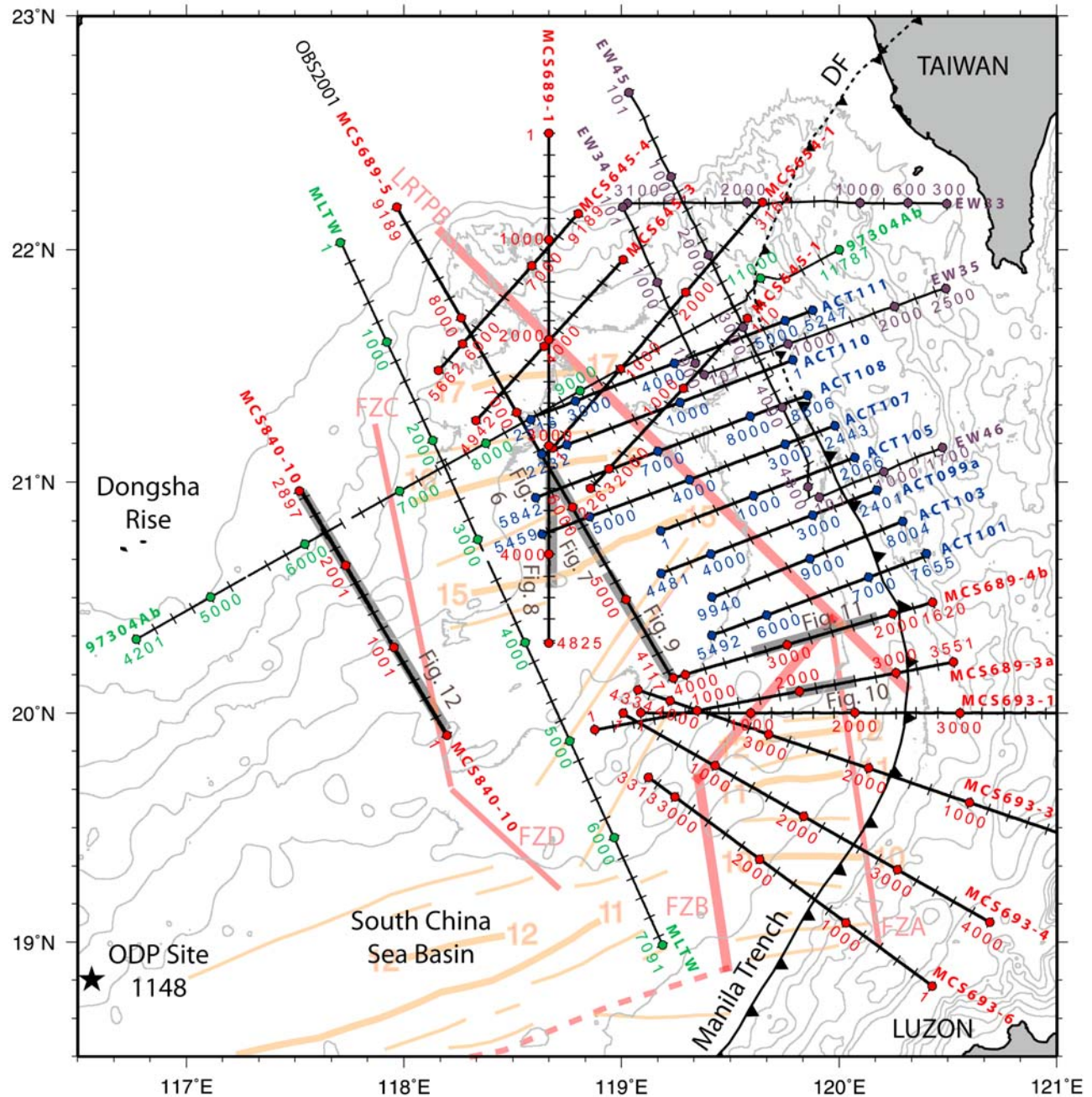
Figure 5. Track lines of multichannel seismic data used in this study. Thin tick marks every 200 shotpoints (SPs) and color circles every 1000 SPs. Bold gray lines with indications of figure numbers are sections of seismic profiles shown in the following figures. Color annotations refer to the research vessels: red, R/V *Ocean Researcher I* (MCS645, 689, 693 and 840–10); blue, R/V *L'Atalante* (ACT cruise); purple, R/V *Maurice Ewing* (EW 9509 cruise), and green, Mainland China research vessel (profiles MLTW and 97304 Aa and Ab). Dimmed magnetic lineations and FZs as in Figure 2. Same legend definitions as in Figure 2.

trends [*Yeh*, 2006] (Figure 13), which could be oceanic spreading or FZ features.

3.3. Acoustic Unconformity U1

[18] Figure 6b is a close-up of a portion of profile MCS689-5 (Figure 6a), which displays a typical tilted fault block characteristic of extensional processes. The acoustic unconformity U1 corresponds to the top of the sedimentary sequence S1 of constant thickness (~0.5 s twt) above

the tilted block and is characterized by overlying onlap reflectors. Thus, a portion of the oceanic crust and its overlying sedimentary sequence has been tilted along a listric basement fault in response to extensional processes. Inside the sedimentary sequence S1 overlying the tilted block, seismic reflectors are parallel to the flat basement. This means that beneath U1 the sediments of sequence S1 were deposited horizontally on a flat horizontal basement. Over a broader area, sediments of sequence S1 vary in
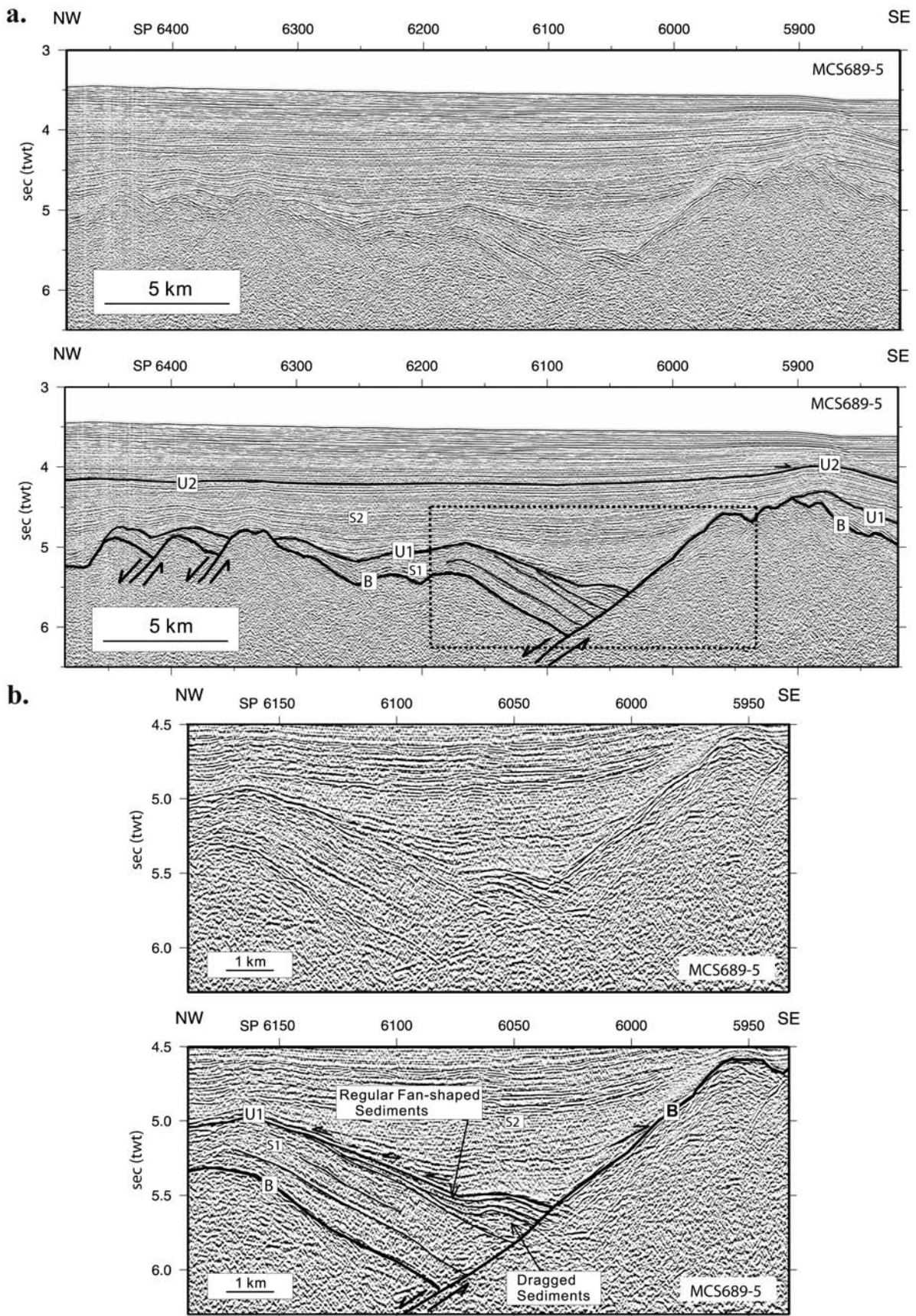
Figure 6
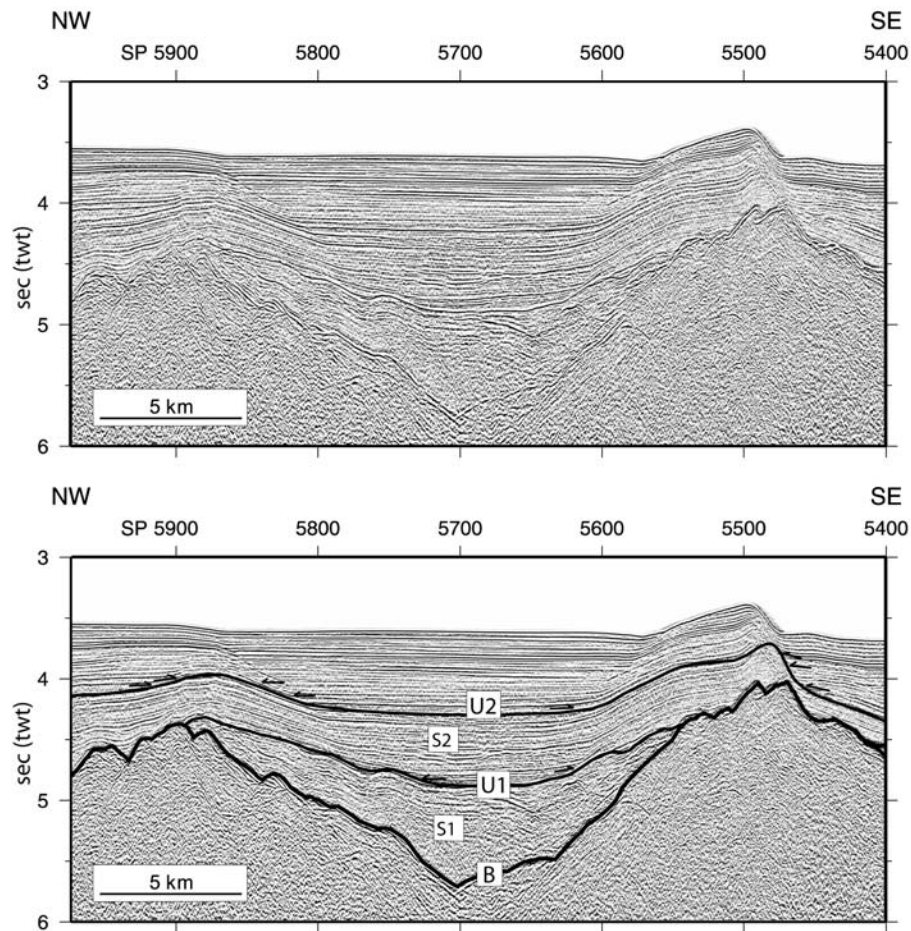
Figure 7. Portion of the seismic profile MCS689-5 located in Figure 5 and showing the U1 and U2 acoustic unconformities. Same legend definitions as in Figure 6.

thickness along the profile and fill up the bathymetric depressions (Figure 6a). They might have a turbiditic origin and probably came from the northern SCS margin.

[19] Above the series of parallel reflectors, fan-shaped reflectors are observed (Figure 6b). Sediments thicken from the crest of the tilted block (shotpoint (SP) 6160) in the direction of the footwall (SP 6050). Dragged sediments next to the footwall might exist in the deepest part of the fan-shaped series. Because the maximum thickness of fan-shaped sediments over the dragged sediments does not exceed 0.2 s twt, the block rotation and the offset along the listric basement fault were rapidly acquired, and from a geological point of view, the extensional phase that we call T1 must be considered a very short event.

[20] Several examples of such tilted fault blocks appear in Figure 6a near SP 6400 and Figure 8 near SP 3600. However, the sedimentary sequence S1 is sometimes very thin, and the characteristics of such an extensional phase cannot be evidenced (e.g., Figure 9). In Figure 11, the S1 sequence is more than 0.5 s twt thick (e.g., near SP 2700). Here, the

deformation of the sequence S1 is linked to a late basement uplift. Profile-to-profile correlations show that normal faults, which were active during the T1 extensional phase, follow spreading directions. This is not surprising, as *Srivastava and Keen* [1995] and *Keen et al.* [1994] demonstrated that extensional processes in the Labrador Sea occurring within the already formed oceanic crust have reactivated spreading directions. Thus, we assume that even if the total amount of extension is on the order of a few kilometers for the whole northeastern SCS, that extension might have taken place perpendicularly to spreading directions as also emphasized by the general distribution of S1 deposits (green areas in Figure 14), which are roughly parallel to identified magnetic lineations. Similarly, green areas located southeast of chron C15 are NE–SW oriented, that is, parallel to the C15− to C12+ magnetic lineations. Close to the Manila trench, the sedimentary sequence S1 is either extremely thin or not identified on the seismic profiles, because the sedimentary thickness considerably increases in the direction of the Manila trench.

Figure 6. (a) Portion of the seismic profile MCS689-5 located in Figure 5 and showing an example of the tensional tectonic phase. U1 and U2 are acoustic unconformities; B, oceanic basement horizon; S1, sedimentary sequence deposited before U1; S2, sedimentary sequence deposited before U2; SP, shotpoint. (b) Detail showing a tilted block, overlying synrotational fan-shaped sediments and onlap features (small arrows).
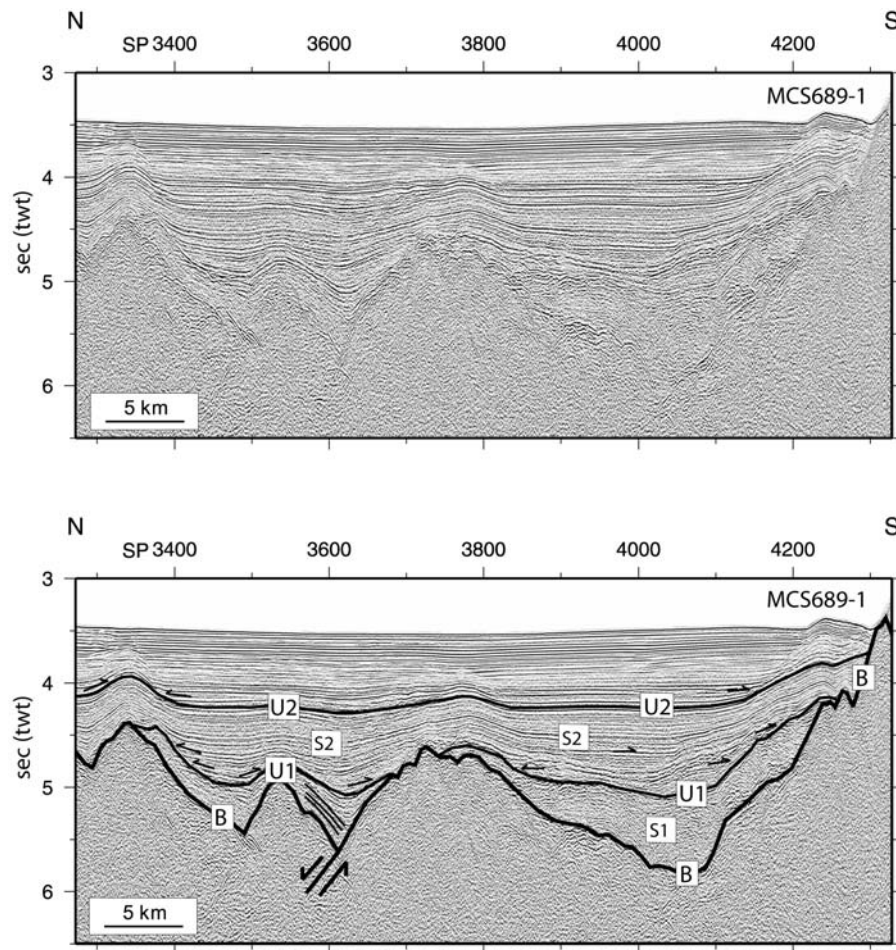
Figure 8. Portion of the seismic profile MCS689-1 located in Figure 5 and showing the U1 and U2 acoustic unconformities. Note the presence of a tilted block and its bounding normal fault at SP 3500. Same legend definitions as in Figure 6.

[21] Magnetic trends and geological features appear on the S1 distribution map of northern SCS (Figure 14). The lateral extension of the LRTPB, considered as an active plate boundary from late Cretaceous to 17–18 Ma [Sibuet et al., 2002], corresponds to the hachured area and is symbolized by a straight thick line. As the geographical distribution of S1 is restricted to SW of the LRTPB, the LRTPB was an active plate boundary at the time of the T1 tectonic phase and the SCS stress regime was not transmitted across the LRTPB.

3.4. Acoustic Unconformity U2

[22] The acoustic unconformity U2 is characterized by overlying onlap reflectors and is associated with the uplift of volcanic ridges (Figures 7, 8, 9, 10, 11, and 12). Figures 7 and 8 show examples of ridges which have been slightly uplifted, with their overlying sediments belonging to the S1 and S2 sedimentary sequences. When ridges have a bathymetric expression, the swath-bathymetric data were used to define their trends. For example, at SP 4500 in Figure 9, the volcanic body corresponds to a ridge on the bathymetric map but also on seismic data as the seafloor is at different depths on each side of this feature, suggesting that the ridge plays the role of damming the sediments deposited. This ridge is oriented NE–SW (Figure 13). At SP 5000 (Figure 9), the uplift of oceanic basement is about 0.7 s twt after the deposition of sequence S2. The deformation in sequence S2 is well imaged, and the continuity of reflectors is clear. Onlap features are observed along the deformed flanks, suggesting turbiditic deposition. In the upper part of the sedimentary section, there is a gradation between pelagic and turbiditic sediments, which explains why the sedimentary ridge still has a bathymetric expression. At SP 4260 in Figure 8, the volcanic ridge, which was uplifted after the deposition of sequence S2, presents a bathymetric expression corresponding to an ENE–WSW direction (Figure 13). In Figure 10, the S2 sedimentary sequence is poorly layered, except in its southwestern part, where faint reflectors parallel to the top of the sequence show that the S2 sequence was deposited in a flat environment before the uplift. In Figure 11, the three ridges at SP 3200, 2600, and 2200 are uplifted after the deposition of sequence S2, but the largest uplift affected the central ridge, which corresponded to the deepest part of the basin before the uplift. On this profile, sediments of sequence S1 were only slightly affected by the T1 phase of extension.

[23] Figure 12 shows the seismic profile MCS840–10 shot in 2007 across the northern SCS margin (location in
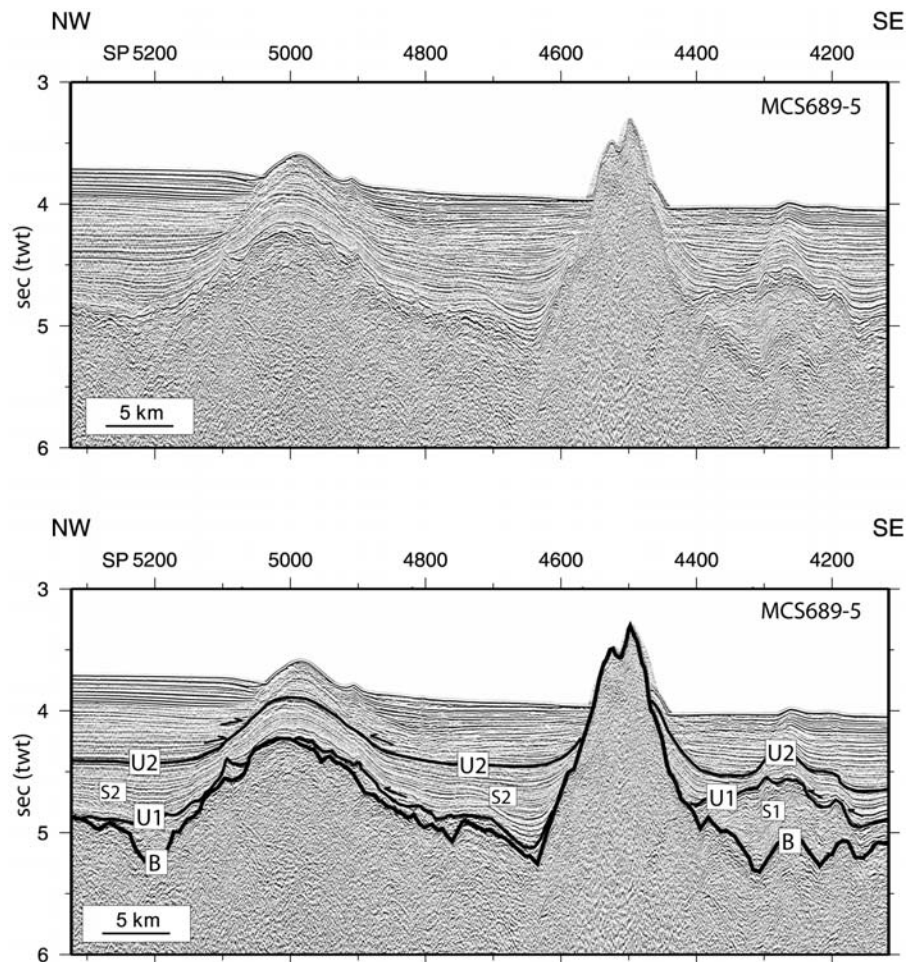
Figure 9. Portion of the seismic profile MCS689-5 located in Figure 5 and showing the U1 and U2 acoustic unconformities. Same legend definitions as in Figure 6.

Figure 5). In contrast with profiles shot across the portion of margin located north of the LRTPB (e.g., R/V *Maurice Ewing* profile EW45 located in Figure 5 and reproduced by *Sibuet et al.* [2002]), this profile shows tectonic features in the distal part of the continental margin. At its southern extremity, the basement was uplifted as well as the overlying sediments along a fault dipping landward on its northwestern side. The two positive features located between SP 0–500 and SP 500–1000, even if they seem to be bounded landward by a normal fault, are uplifted with respect to the rest of the profile. This is confirmed by old Lamont profiles (Vema 3608) shot in the close vicinity, where the same two positive features replaced in a more general context clearly show uplifted features at the base of the continental margin. Adjacent to the main fault at SP 1000, part of the deformation in the sediments might correspond to dragged sediments by the motion along the fault. Other profiles shot during the same cruise in the vicinity of Profile MCS840–10 also display uplifted features, with some of them being located much higher on the continental slope.

[24] Figure 15 shows the spatial distribution of deformed sediments and uplifted ridges after the deposition of sedimentary sequence S2. All deformed sediments are located south of the LRTPB, from the northeastern SCS margin to the Manila trench, except perhaps in a restricted area located

north of chrons C10 to C12. The deformation might extend southwest of our study area as shown by the southwestward extension of some bathymetric features (Figure 2), but this possibility is not yet confirmed in this study, even though the deformation is observed on the continental margin south of Dongsha Rise.

4. Discussion

4.1. Basement Provinces

[25] Figure 16 maps the crustal provinces of the northeastern SCS. As previously established, the age of the oldest oceanic crust identified by the presence of magnetic lineations decreases from east to west, i.e., from chron C17 (37.8 Ma) to chron C5c (16.7 Ma) [*Hsu et al.*, 2004; *Briais et al.*, 1993]. North of the LRTPB, the extreme northeastern part of the SCS, called the Proto-SCS plate in this study, may belong to a different plate (Proto-SCS or Philippines Sea plate) [*Sibuet et al.*, 2002] from the rest of the SCS. Though the age of the Proto-SCS plate is unknown, the mean depth of the oceanic basement in the area of the three ridges is at least 0.8 km deeper than that south of the LRTPB (Figure 13), suggesting that this portion of oceanic plate is much older than chron C17 (37.8 Ma).
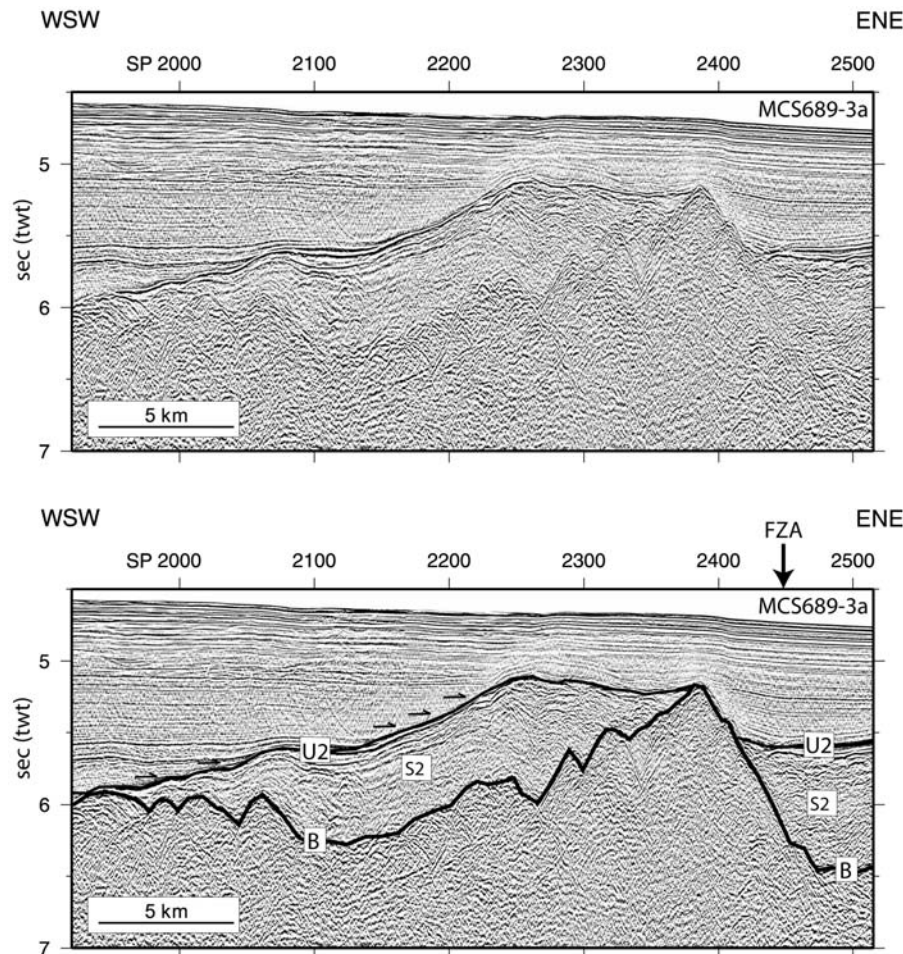
Figure 10. Portion of the seismic profile MCS689–3a located in Figure 5 and showing the U2 acoustic unconformity. Note the thick deformed S2 sedimentary sequence between SP 2000 and SP 2400. Same legend definitions as in Figure 6.

[26] South of chron C15 (35 Ma), in the yellow triangular domain, magnetic anomalies are faint (Figure 16). However, basement ridges are still parallel to chrons C15 to C17, suggesting that this yellow triangular domain still belongs to the C17-C15 ENE–WSW trending yellow domain. The orange domain located immediately to the southeast is characterized by NE–SW oriented basement ridges and weak magnetic lineations. It seems reasonable to infer that the orange oceanic domain was created sometime between chrons C15− and C12+. In the absence of southern conjugate portions of both the yellow and orange domains as well as the C12+ to C10− green domain located between FZA and FZB, which have subducted beneath the Manila subduction zone [*Sibuet et al.*, 2004], we assume that the subducted portions of the yellow, orange, and green domains were formed symmetrically and that half-spreading rates computed in the northeastern SCS are half values of full spreading rates (Figure 3).

[27] South and west of the orange domain, magnetic lineations C12+ and younger are again parallel to the northern SCS margin trend and bounded by fracture zones FZA, FZB, and FZD. FZA limits the eastern prolongation of N085° magnetic lineations C12+ to C10−. FZB accommodates both the 45° change in spreading directions from

the orange to the green domain located southeast and the change in directions of magnetic lineations C12+ to C10− from N085° east of FZB to N075° west of FZB, suggesting that FZB is not only a FZ but also a plate boundary during the C12+ to C10− period. In this scheme, the northern limit of the green domain between FZB and LRTPB is also a plate boundary, and a ridge jump might have occurred at the time of chron C13+. FZE prolongs to the north the eastern extension of Macclesfield Bank and limits to the east the formation of a small symmetrical basin created between Macclesfield Bank and the margin [*Briais et al.*, 1993], suggesting that FZE is a plate boundary. The trend of FZE is badly constrained.

[28] The boundary between the green and light blue domains is not an isochron. It accommodates the progressive westward change of spreading directions from N075° between FZB and FZE, to E–W south of it (Figure 1). This change occurs between chrons C10+ and C9. The change of spreading directions during the chrons C7+ to C6b period coincides with a ridge jump to the south [*Briais et al.*, 1993]. Similarly, the boundary between the light and dark blue domains accommodates, east of 117.5°E, a 30° change of spreading directions from E–W to N060° during the chrons
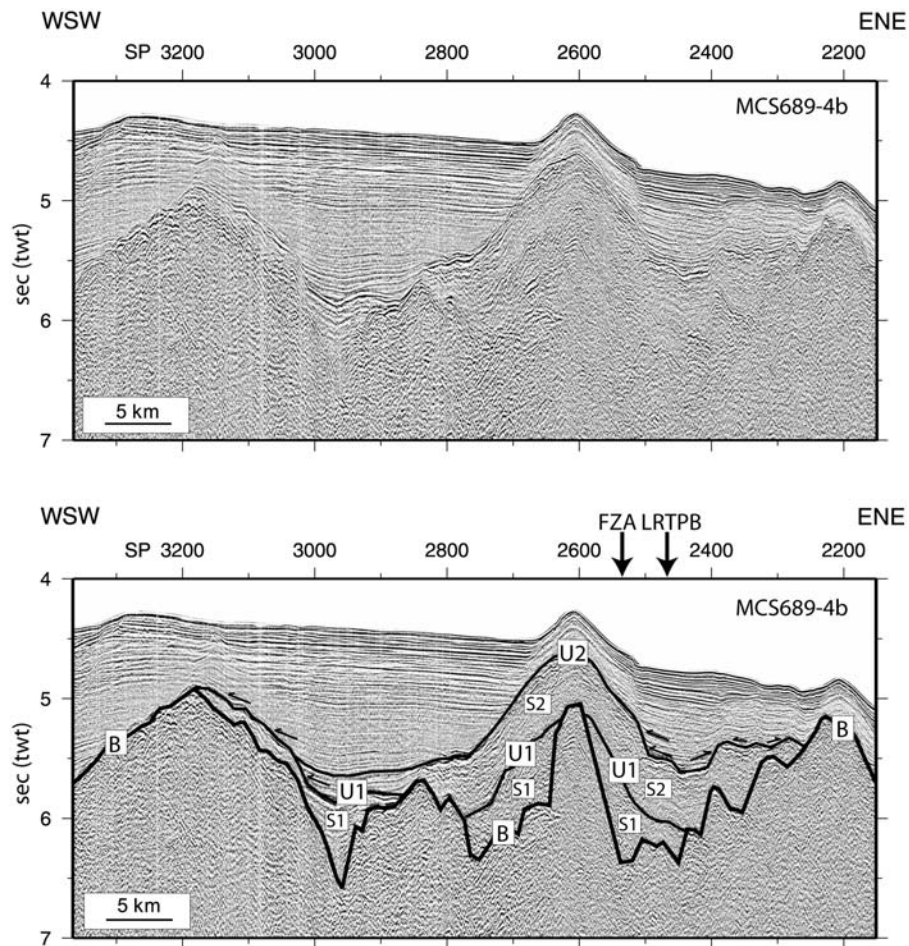
Figure 11. Portion of the seismic profile MCS689–4b located in Figure 5 and showing the U2 acoustic unconformity. Same legend definitions as in Figure 6.

C7+ to C6b− period, suggesting that a ridge readjustment occurred west of 117.5°E longitude.

[29] The main input of this study is the discovery of a major 45° change in spreading directions during the chrons C15− to C12+ period, which might be the consequence of the significant rotation of a very small plate located between the adjacent large Philippine Sea and Eurasia plates [*Sibuet et al.*, 2002]. In addition, the changing geometry of small plates formed during the creation of the yellow and orange domains, even though during the creation of the C12+ to C10 green domain, may also depend on the relative motions of large surrounding plates.

4.2. Extensional Phase T1

[30] Because of the presence of tilted fault blocks (e.g., Figure 6), the T1 tectonic phase is clearly extensional. Several arguments can be used to constrain the age of the tectonic phase T1. They include the age of the youngest oceanic crust affected by T1, drilling data at Ocean Drilling Program (ODP) Site 1148 on the northern SCS margin, industry seismic data collected west of Taiwan and well subsidence curves obtained in west Taiwan continental shelf basins [*Lin et al.*, 2003].

[31] The youngest oceanic domain affected by the extensional phase T1 is where chron C11 (30.1 Ma) has been identified (Figure 14). It means that the tectonic phase T1 is younger than 30.1 Ma. At ODP Site 1148 drilled in the lower part of the northern SCS continental margin in 3294 m water depth (Figure 14), a hiatus was found at 470 m below the seafloor, at the Oligocene/Miocene boundary. This hiatus lies between 25 and 28.5 Ma or 26 and 28.5 Ma on the basis of foraminiferal or nanofossil data [*Prell et al.*, 2006], respectively. On the seismic section, this hiatus corresponds to an unconformity with onlap reflectors on top of it. The sedimentation rates vary from 55 m/Ma below the hiatus to 15 m/Ma above. A thin mass flow or a series of slumps was cored above the hiatus, with clear evidence of normal faulting likely related to a change in the tectonic activity in the SCS [*Prell et al.*, 2006]. Even if there is no major variation in half-spreading rates at the time of chrons C9 (27.9 Ma) to C11 (30 Ma), we have identified a major change in spreading directions (Figures 1 and 3) during this period, which corresponds to the age of the ODP Site 1148 hiatus.

[32] Seismic profile R, not reproduced in this paper, is located southwest of ODP Site 1148 [*Taylor and Hayes*, 1983] and between chron C9 (27.9 Ma) and C10 (28.7 Ma)
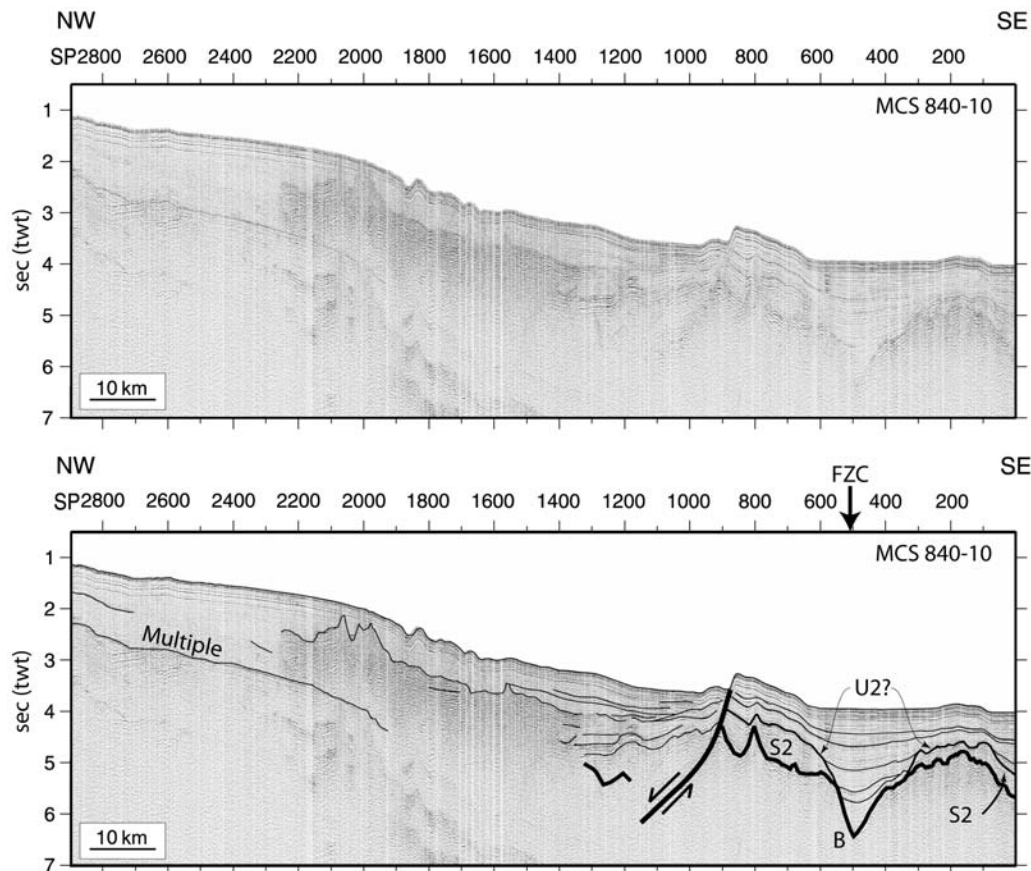
Figure 12. Seismic profile MCS840-10 located in Figure 5 and showing a possible compressive deformation linked to the U2 acoustic unconformity and located at the base of the northeastern SCS margin.

(Figure 1). It shows a strong reflector observed a few tens of meters above the basement. Onlap reflections on top of this reflector demonstrate that it corresponds to the base of an unconformity that we correlate with the ODP Site 1148 hiatus of the same age, showing that tectonic phase T1 affected the already formed SCS.

[33] Industry seismic profiles shot in the west Taiwan basins show that the major unconformity dated 37 Ma from wells data [*Lin et al.*, 2003] corresponds now to the onset of oceanic crust in the northeastern SCS (chron C17, 37.8 Ma), and possibly to the breakup unconformity as established by *Hsu et al.* [2004] and *Sibuet et al.* [2004]. Another major unconformity, less significant than the breakup unconformity, is dated ~30 Ma. Initially associated by *Lin et al.* [2003] with the onset of spreading in the northern SCS at 30 Ma, we suggest that this unconformity is instead linked to the extensional phase T1 associated with the northeastern SCS change in spreading direction occurring around chron C10 (~28.7 Ma).

[34] Thus, the age of the extensional phase T1 is quite well constrained: younger than 30.1 Ma from the distribution of T1 deformation in the northeastern SCS, 25–28.5 Ma from ODP Site 1148, 27.9–30.1 Ma for the main change in spreading directions in northeastern SCS, and finally ~30 Ma from seismic and wells data obtained in the west Taiwan basins. Consequently, the tectonic phase T1 might have occurred ~28–30 Ma (middle Oligocene).

4.3. Magmatic Phase T2

[35] We have seen that the U2 unconformity is associated with an uplift of the northeastern SCS volcanic ridges. This uplift reactivated preexisting spreading features and is either due to a magmatic event or to a compressive event approximately oriented perpendicularly to the spreading directions, i.e., in the NNW–SSE to NW–SE direction. On almost all the uplifted ridges, we cannot find evidence for any sign of compression. There are no folds or reverse faults associated with the uplifted ridges, except in Figure 12, where the fault at SP 1000 might be a reverse fault where the basement high between SP 500 and 1000 might eventually be uplifted with respect to the rest of the seismic section. We consequently suggest that the U2 unconformity was not created by a compressive event but was due to a generalized magmatic episode, which uplifted the former spreading features and seamounts belonging to the portion of northeastern SCS located SW of the LRTPB and mapped in Figure 15. The reverse fault of Figure 12 would have been generated by a significant uplift of the block located between SP 500 and 1000 consecutive to this magmatic event. As there is no information available from drilling, it is difficult to date this magmatic event. However, a basaltic dredge sample collected from a large seamount located on or close to the LRTPB at 21°10′N; 119°12′E (Figure 5) is dated 22 Ma [*Hsu et al.*, 2004], suggesting that the T2 magmatic
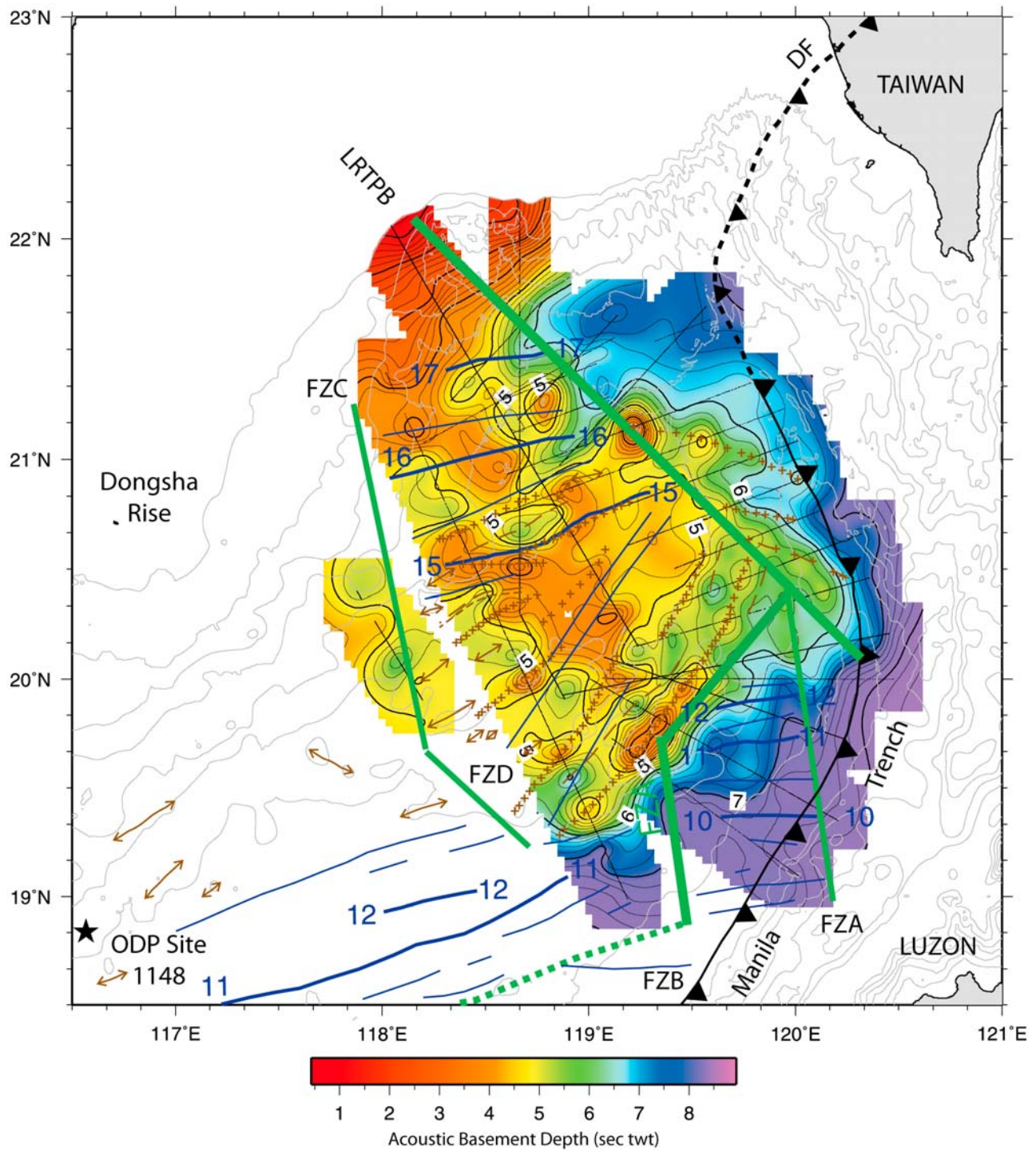
Figure 13. Basement map established from available seismic data of Figure 5. The basement is of oceanic nature in the deep abyssal domain and of continental nature beneath the northeastern SCS continental margin. Track lines are shown only where the basement has been identified. Thin gray lines, 500 m bathymetric contours. Magnetic lineations are shown in dark blue. Thin green lines, FZs; thick green lines, plate boundaries; green dashed lines, changes in seafloor spreading directions; black crosses and dashed black lines, structural highs and depressions established from seismic data, respectively; black lines with double arrows, ridge axes determined from bathymetric data. DF, deformation front.
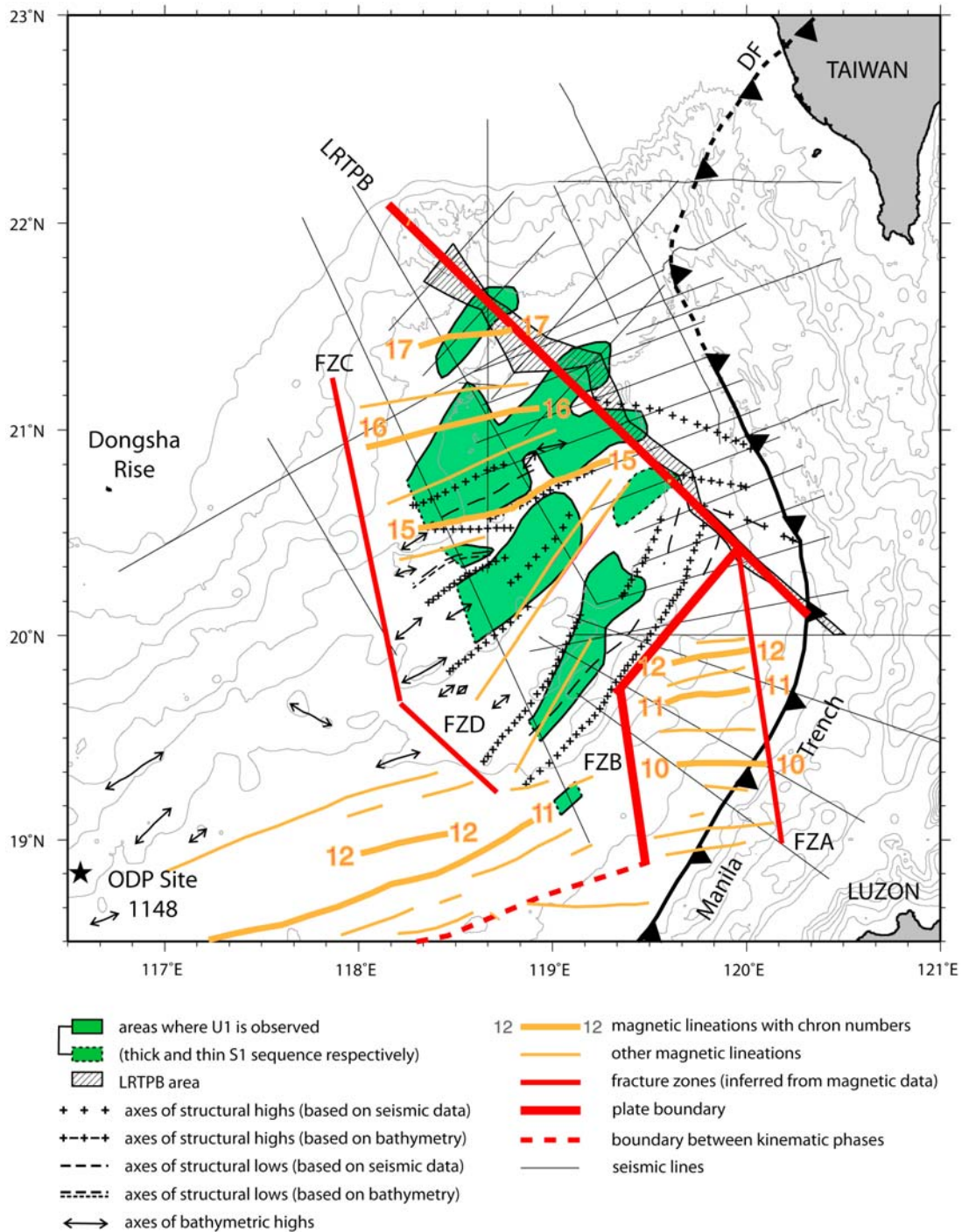
Figure 14. Spatial distribution of U1 acoustic unconformity associated with the extensional phase T1. Note the absence of T1 deformation north of the LRTPB. Same legend definitions as in Figure 2.

phase occurred during the early Miocene, before the end of the SCS opening.

4.4. Kinematic Model

[36] On the basis of the identification of magnetic lineations in the northeastern SCS and variations in spreading rates, we were able to define the principal phases of formation of the SCS oceanic domain. The onset of oceanic domain started 37.8 Ma ago (chron C17). From seismic profiles, we have defined the existence of two phases, which occurred during the formation of the SCS. The first one, T1, is a tensional phase, which occurred 28–30 Ma ago, ~8–10 Ma after the onset of seafloor spreading in the northeastern SCS. A significant amount of already deposited sediments (maximum 0.8 s twt) recorded the deformation, and fan-shaped deposits attest to the rotation of oceanic basement
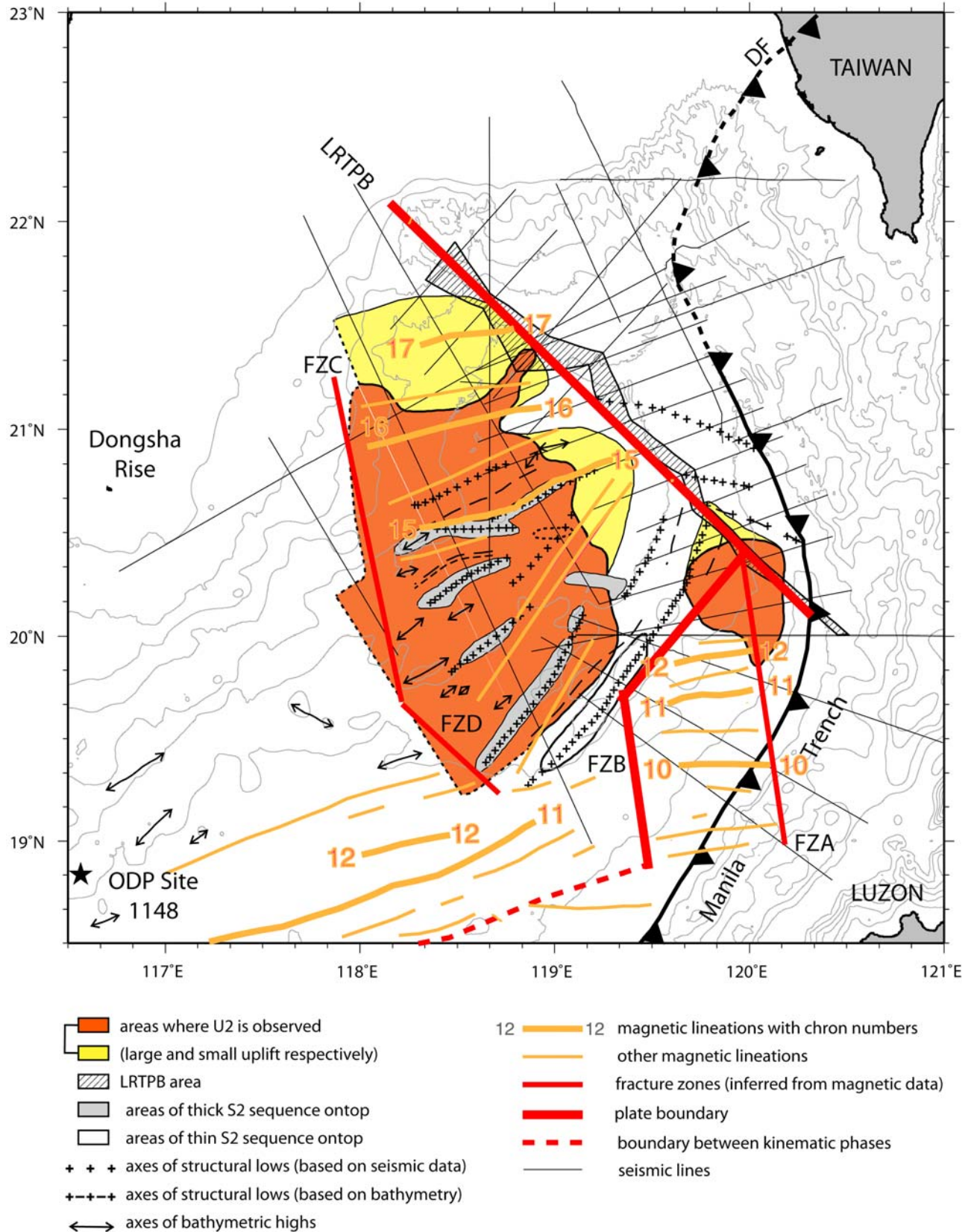
Figure 15. Spatial distribution of U2 acoustic unconformity associated with the T2 magmatic phase. Note the absence of uplift north of the LRTPB. Same legend definitions as in Figure 2.
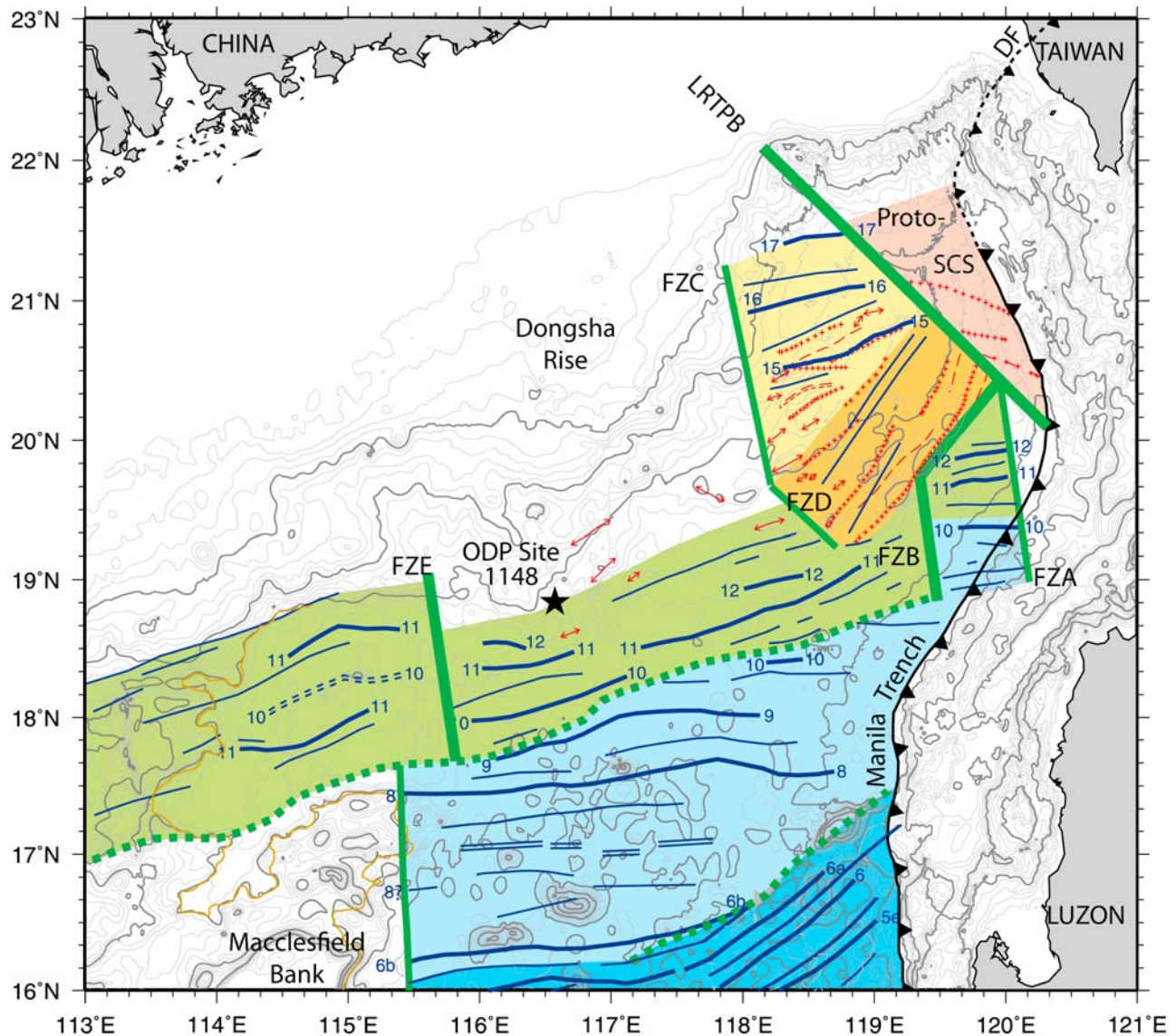
Figure 16. Kinematic framework of the northeastern SCS. Bathymetry every 200 m in gray and every 1000 m in dark gray. Dark blue lines, magnetic lineations; double dark blue dashed lines, failed rift axes; thick green lines, FZs; thick green lines, plate boundaries; dotted thick green lines, boundary between kinematic phases; red crosses and dashed red lines, structural highs and depressions established from seismic data, respectively; red lines with double arrows, ridge axes determined from bathymetric data. Note that there is a good fit between structural trends and magnetic lineations. Light pink, oldest oceanic domain in the SCS belonging either to the Philippine Sea plate or to the Proto-SCS plate. Colors represent oceanic domains formed between significant tectonic phases marked by changes in spreading rates, spreading directions or both (Figure 8): yellow, chron C17 to C15− oceanic domain formed perpendicularly to the direction of the portion of continental margin located north of the LRTPB with seafloor spreading extension at azimuth N166°; orange, chron C15− to C12+ oceanic domain formed during a short period of time with seafloor spreading extension at azimuth N135°. Light green, chron C12+ to C9/C10 oceanic domain formed again perpendicularly to the direction of the continental margin north of the LRTPB with seafloor spreading extension at azimuth N164°. Light blue, chron C9/C10 to C6b oceanic domain formed at azimuth N180°. Dark blue, chron C6b to 15.5 Ma oceanic domain formed at azimuth N150° in its eastern part and at azimuth N180° in its western part, suggesting that a rift axis readjustment occurred at chron C6b west of 117.5°E longitude.

blocks during this tensional phase. Though the duration of this tensile episode is not known yet, it was probably a short one, on the order of 1–2 Ma. Figure 17a shows the kinematic reconstruction at the time of chron C10 (28.7 Ma).

The SCS was <500 km wide and the southern part of the Proto-SCS plate was probably lying south as well as east of it [*Clift et al.*, 2008]. The Proto-SCS plate was subducting beneath Borneo and Palawan, and the Celebes Sea was
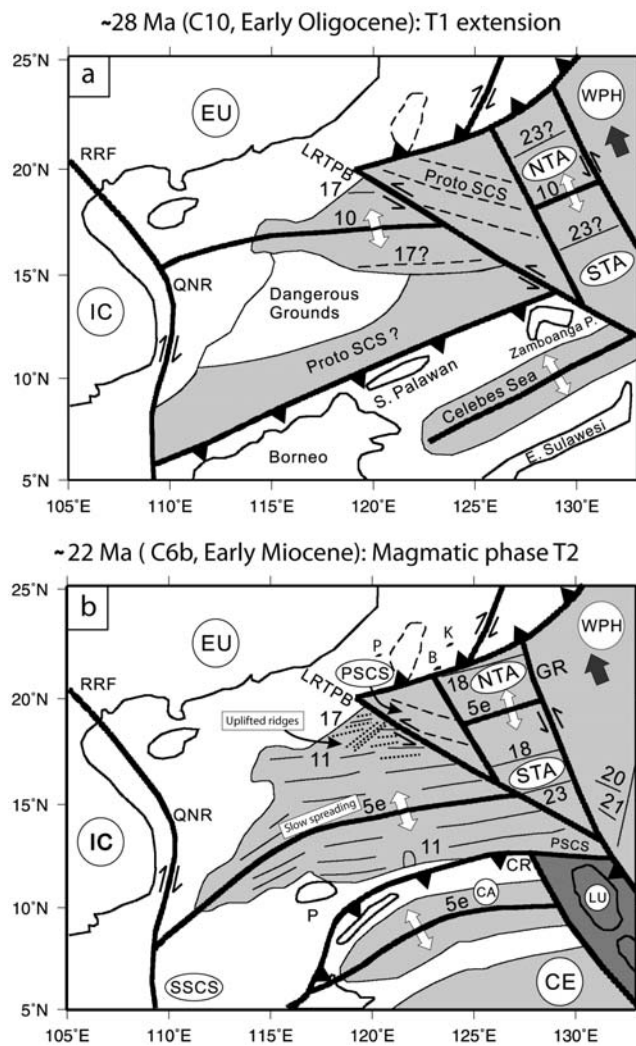
Figure 17. Plate kinematic models showing the geodynamic evolution of the SCS region adapted from *Sibuet et al.* [2002]. (a) At chron C10 (~28 Ma), the time of T1 tensional deformation. (b) At ~22 Ma (~chron C6b), the time of the magmatic event with uplift of former spreading features. Light gray, oceanic domain; dark gray, Luzon arc; thick lines, active plate boundaries; large arrows, WPH/EU motion; B and K, locations of Baolai and Kungkuan early Miocene alkali basalts before Taiwan uplift; CR, Cagayan Ridge; GR, Gagua Ridge; MT, Manila Trench; LU, Luzon plate; P, Palawan; QNR, Qui Nhon Ridge; RRF, Red River Fault; CA, Cagayan plate; CE, Celebes plate; EU, Eurasia continental plate; IC, Indochina plate; NTA, north Taiwan Sea plate; P, Penghu Islands; PSCS, Proto-South China Sea plate; SSCS, southern South China Sea plate; STA, south Taiwan Sea plate; WPH, west Philippine Sea plate.

opening behind the subduction zone system. A major change in the direction of spreading occurred at chrons C9–C10 (27.9–28.7 Ma) (Figure 1), but with a minor change in spreading rates (Figure 3). However, at chron C12 (31 Ma), a big change in spreading rate occurred without significant change in spreading direction. Modifications in the parameters of plate convergence (e.g., slab dip) may change the

stress pattern in the plate, which subducts beneath Borneo and Palawan, allowing the possibility to increase the tensional stress into the adjacent oceanic crust, resulting in a change of direction of spreading or spreading rate and potential intraplate deformation.

[37] The magmatic phase T2 occurred during the early Miocene before the end of the SCS opening. It was observed only southwest of the LRTPB, suggesting that the LRTPB was an active feature at the time of the magmatic phase. The LRTPB either acted as a barrier to the northward propagation of the magmatic event or, if magmatic manifestations occurred north of the LRTPB, was subducted beneath the Eurasia plate. Figure 17b shows the kinematic reconstruction at 22 Ma. The subduction was ongoing along the Ryukyu subduction system east of the LRTPB but also in the southwestern SCS, where the Proto-SCS plate was subducting beneath Palawan. The Cenozoic extension in the Taiwan region resulted in intraplate basaltic volcanism during the early Miocene (23–20 Ma), with eruption of alkali basalt only [*Yen*, 1958]. They are represented by alkali basalts of the Kungkuan region located in the northwest of Taiwan, south of the Taitun volcano and possibly by the Baolai alkali basalts, though their early Miocene age is not firmly established [*Smith and Lewis*, 2007]. At the time of their emplacement, the Kungkuan and Baolai volcanics were located ~200 km southeast of the present-day position of Taiwan (Figure 17b). The early Miocene Kungkuan basalts present homogeneous Sr-Nd-Pb isotopic composition [*Chung et al.*, 1995] similar to that of our SCS dredge sample (S.-L. Chung, personal communication, 2009), suggesting that the early Miocene basalts of northwest Taiwan (Kungkuan), south-central Taiwan (Baolai), and our SCS basaltic sample belong to the same magmatic province because of their contemporaneous eruption ages and the close spatial relationship and elemental similarities [*Chen et al.*, 2001; *Chung et al.*, 1995] (Figure 17b). *Chung et al.* [1995] proposed that decompression melting of the convective mantle intermingling with EM2-type "plums" in the basal lithospheric mantle produced the early Miocene alkali basalts in the Kungkuan region. On the basis of the major trace elements and isotopic compositions of the Kungkuan and of the basalts dredged in the northeastern SCS being similar, we suggest that a large early Miocene intraplate magmatic province existed, comprising the northeastern SCS uplifted ridges (Figure 15), northern Taiwan, and south-central Taiwan. We cannot exclude that the magmatic phase might extend during the middle Miocene as the middle Miocene Penghu basalts (Figure 17b) present trace elements and isotopic compositions indistinguishable from the Kungkuan, Baioli, and our northern SCS dredged basalt [*Chen et al.*, 2001; *Chung et al.*, 1995; *Smith and Lewis*, 2007].

5. Conclusions

[38] The main conclusions of this study are as follows:
[39] 1. The northeastern SCS basin opened via seafloor spreading from chron C17 (37.8 Ma) to 15.5 Ma (after chron C5c, 16.7 Ma) with several kinematic phases from (1) C17 (37.8Ma) to C15− (<35 Ma) with spreading directions parallel to the general trend of the northern SCS margin, (2) C15− (<35 Ma) to C12+ (>31 Ma) with spreading

directions trending N045°, and (3) C12+ (>31 Ma) to C10/C9 (27.9/28.7 Ma) with spreading directions again parallel to the general trend of the northern SCS margin. FZs and plate boundaries define the limits of these oceanic crustal domains.

[40] 2. The tectonic phase T1 is a minor tensional phase which occurred 28–29 Ma ago. This event is characterized by the tilting of oceanic basement fault blocks and the formation of fan-shaped reflectors identified from seismic data in the northeastern SCS, south of the LRTPB.

[41] 3. The magmatic phase T2 occurred ~22 Ma ago. Former spreading features were uplifted in the deep northeastern SCS basin, south of the LRTPB, which was still an active plate boundary at that time. Simultaneously, early Miocene (20–23 Ma) alkali basalts were emplaced in north and south-central Taiwan, suggesting that a generalized intraplate magmatic episode occurred at that time in Southeast Asia.

References

Barckhausen, U., and H. A. Roeser (2004), Seafloor spreading anomalies in the South China Sea revisited, in *Continent-Ocean Interactions Within East Asian Marginal Seas, Geophys. Monogr. Ser.*, vol. 149, edited by P. Clift et al., pp. 121–125, AGU, Washington, D. C.

Bowin, C. O., R. S. Ru, C. S. Lee, and H. Schouten (1978), Plate convergence and accretion in Taiwan-Luzon region, *Am. Assoc. Pet. Geol. Bull.*, 62, 1645–1672.

Briais, A., P. Patriat, and P. Tapponnier (1993), Updated interpretation of magnetic anomalies and seafloor spreading stages in South China Sea: Implications for the tertiary tectonics of Southeast Asia, *J. Geophys. Res.*, 98, 6299–6328, doi:10.1029/92JB02280.

Bullock, A. D., and T. A. Minshull (2005), From continental extension to seafloor spreading: Crustal structure of the Goban Spur rifted margin, southwest of the UK, *Geophys. J. Int.*, 163, 527–546, doi:10.1111/j.1365-246X.2005.02726.x.

Cande, S. C., and D. V. Kent (1995), Revised calibration of the geomagnetic polarity timescale for the Late Cretaceous and Cenozoic, *J. Geophys. Res.*, 100, 6093–6095, doi:10.1029/94JB03098.

Chen, S. (1987), Magnetic profiles, in *Atlas of Geology and Geophysics of the South China Sea*, scale 1:2,000,000, Second Mar. Geol. Invest. Brigade of the Minist. of Geol. and Miner. Resour., Guangdong, China.

Chen, C.-H., S.-H. Chung, H.-H. Wang, C.-H. Chen, and S.-L. Chung (2001), Petrology and geochemistry of Neogene continental basalts and related rocks in northern Taiwan (III): Alkali basalts and tholeiites from Shiting-Yinko area, *West. Pac. Earth Sci.*, 1, 19–46.

Christensen, N. I., and W. D. Mooney (1995), Seismic velocity structure and composition of the continental crust: A global view, *J. Geophys. Res.*, 100, 9761–9788, doi:10.1029/95JB00259.

Chung, S.-L., B.-M. Jahn, S.-J. Chen, T. Lee, and C.-H. Chen (1995), Miocene basalts in northwestern Taiwan: Evidence for EM-type mantle sources in the continental lithosphere, *Geochim. Cosmochim. Acta*, 59, 549–555, doi:10.1016/0016-7037(94)00360-X.

Clift, P., G. H. Lee, N. Anh Duc, U. Barckhausen, H. Van Long, and S. Zhen (2008), Seismic reflection evidence for a Dangerous Grounds miniplate: No extrusion origin for the South China Sea, *Tectonics*, 27, TC3008, doi:10.1029/2007TC002216.

Gradstein, F. M., J. G. Ogg, and A. G. Smith (2004), *A Geologic Time Scale 2004*, 589 pp., Cambridge Univ. Press, Cambridge, UK.

Geological Survey of Japan and Coordinating Committee for Geoscience Programmes in East and Southeast Asia (1994), Magnetic Anomaly Map of East Asia, edited, Miscellaneous Map Series 32.

Hsu, S.-K., Y.-C. Yeh, W.-B. Doo, and C.-H. Tsai (2004), New bathymetry and magnetic lineations in the northernmost South China Sea and their tectonic implications, *Mar. Geophys. Res.*, 25, 29–44, doi:10.1007/s11001-005-0731-7.

Keen, C. E., P. Potter, and S. P. Srivastava (1994), Deep seismic reflection data across the conjugate margins of the Labrador Sea, *Can. J. Earth Sci.*, 31, 192–205, doi:10.1139/e94-016.

Ku, C.-Y., and S.-K. Hsu (2009), Crustal structure and deformation at the northern Manila Trench between Taiwan and Luzon islands, *Tectonophysics*, 466, 229–240, doi:210.1016/j.tecto.2007.1011.1012.

LaBrecque, J., D. V. Kent, and S. C. Cande (1977), Revised magnetic polarity time scale for Late Cretaceous and Cenozoic time, *Geology*, 5, 330–335, doi:10.1130/0091-7613(1977)5<330:RMPTSF>2.0.CO;2.

Lin, A. T., A. B. Watts, and S. P. Hesselbo (2003), Cenozoic stratigraphy and subsidence history of the South China Sea margin in the Taiwan region, *Basin Res.*, 15, 453–478, doi:10.1046/j.1365-2117.2003.00215.x.

Maus, S., et al. (2005), The 10th-Generation International Geomagnetic Reference Field, *Geophys. J. Int.*, 161, 561–565, doi:10.1111/j.1365-246X.2005.02641.x.

Mutter, C. Z., and J. C. Mutter (1993), Variations in thickness of layer 3 dominate oceanic crustal structure, *Earth Planet. Sci. Lett.*, 117, 295–317, doi:10.1016/0012-821X(93)90134-U.

National Geophysical Data Center. (2002), *GEODAS CD-ROM worldwide Marine Geophysical Data*, Natl. Oceanic and Atmos. Admin., U.S. Dept. of Commerce, Boulder, CO.

Patriat, P. (1987), *L'évolution du système de dorsales de l'Océan Indien*, 310 pp., Terres Australes et Antarctiques Françaises, Paris.

Peltzer, G., and P. Tapponnier (1988), Formation and evolution of strike-slip faults, rifts and basins during the India-Asia collision: An experimental approach, *J. Geophys. Res.*, 93(B12), 15,085–15,117, doi:10.1029/JB093iB12p15085.

Prell, W. L., P. Wang, P. Blum, D. K. Rea, and S. C. Clemens (2006), Proc. ODP Sci Results 184: Ocean Drill. Program, College Station, Tex.

Sibuet, J.-C., S.-K. Hsu, X. Le Pichon, J.-P. Le Formal, D. Reed, G. Moore, and C.-S. Liu (2002), East Asia plate tectonics since 15 Ma: Constraints from the Taiwan region, *Tectonophysics*, 344, 103–134, doi:10.1016/S0040-1951(01)00202-5.

Sibuet, J.-C., S.-K. Hsu, and E. Debayle (2004), Geodynamic context of the Taiwan orogen, in *Continent-Ocean Interactions Within East Asian Marginal Seas*, edited by P. Clift et al., pp. 127–158, AGU monograph, Washington, D.C.

Smith, A. D., and C. Lewis (2007), Geochemistry of metabasalts and associated metasedimentary rocks from the Lushan formation of the upthrust Slate belt, south-central Taiwan, *Int. Geol. Rev.*, 49, 1–13, doi:10.2747/0020-6814.49.1.1.

Srivastava, S. P., and C. E. Keen (1995), A deep seismic reflection profiles across the extinct Mid-Labrador Sea spreading center, *Tectonics*, 14, 372–389, doi:10.1029/94TC02453.

Tapponnier, P., G. Peltzer, A. Y. Le Dain, R. Armijo, and P. Cobbold (1982), Propagating extrusion tectonics in Asia: New insights from simple experiments with plasticine, *Geology*, 10, 611–616, doi:10.1130/0091-7613(1982)10<611:PETIAN>2.0.CO;2.

Taylor, B., and D. E. Hayes (1980), The tectonic evolution of the South China Sea, in *The Tectonic and Geologic Evolution of Southeast Asian Seas and Islands, Part 1, Geophys. Monogr. Ser*, edited by D. E. Hayes, pp. 89–104, AGU, Washington, D.C.

Taylor, B., and D. E. Hayes (1983), Origin and history of the South China Sea basin, in *The Tectonic and Geologic Evolution of Southeast Asian Seas and Islands, Part 2, Geophys. Monogr. Ser.*, edited by D. E. Hayes, pp. 23–56, AGU, Washington, D.C.

Tsai, C.-H., S.-K. Hsu, Y.-C. Yeh, C.-S. Lee, and K.-Y. Xia (2004), Crustal thinning of the northern continental margin of the South China Sea, *Mar. Geophys. Res.*, 25, 63–78, doi:10.1007/s11001-005-0733-5.

Wang, T.-K., M.-K. Chen, C.-S. Lee, and K. Xia (2006), Seismic imaging of the transitional crust across the northeastern margin of the South China Sea, *Tectonophysics*, 412, 237–254, doi:10.1016/j.tecto.2005.10.039.

White, R. S., D. McKenzie, and K. O'Nions (1992), Oceanic crustal thickness from seismic measurements and rare Earth element inversions, *J. Geophys. Res.*, 97, 19,683–19,715, doi:10.1029/92JB01749.

Yan, P., D. Zhou, and Z. S. Liu (2001), A crustal structure profile across the northern continental margin of the South China Sea, *Tectonophysics*, 338, 1–21, doi:10.1016/S0040-1951(01)00062-2.

Yeh, Y.-C. (2006), Tectonics of the northern South China Sea, *PhD dissertation*, 148 pp, National Central Univ., Chungli, Taiwan.

Yeh, Y.-C., and S.-K. Hsu (2004), Crustal structures of the northernmost South China Sea: Seismic reflection and gravity modeling, *Mar. Geophys. Res.*, *25*, 45–61, doi:10.1007/s11001-005-0732-6.

Yen, T. P. (1958), Cenozoic volcanic activity in Taiwan, *Taiwan Miner. Ind.*, *10*, 1–39.

S.-K. Hsu, Institute of Geophysics, National Central University, 300 Chung-Da Rd., Chung-Li 32001, Taiwan. (hsu@ncu.edu.tw)

C.-S. Liu, Institute of Oceanography, National Taiwan University, 1, Sec. 4 Roosevelt Rd., Taipei 10617, Taiwan.

J.-C. Sibuet, Institute of Applied Geosciences, National Taiwan Ocean University, 2 Pei-Ning Rd., Keelung 20248, Taiwan.

Y.-C. Yeh, Department of Geology and Geophysics, POST 808, University of Hawaii at Manoa, 1680 East-West Rd., Honolulu, HI 96822, USA. (ycyeh@hawaii.edu)